Dynamic User Clustering and Optimal Power Allocation in UAV-Assisted Full-Duplex Hybrid NOMA System

Mayur Katwe, *Graduate Student Member, IEEE*, Keshav Singh, *Member, IEEE*, Prabhat Kumar Sharma, *Senior Member, IEEE*, Chih-Peng Li, *Fellow, IEEE*, and Zhiguo Ding, *Fellow, IEEE*

***Abstract*— This paper investigates unmanned aerial vehicles (UAVs)-assisted full-duplex (FD) non-orthogonal multiple access (NOMA) system based cellular network, aiming to improve overall sum-rate throughput of the system through dynamic user clustering, optimal UAV placement and power allocation. Since each UAV operates in FD mode, self-interference (SI), co-channel interference (CCI), inter-UAV interference (IUI) and intra-node interference (INI) dominate the system's performance. Consequently, we propose an unconventional two-stage dynamic user clustering for user nodes (UNs) to reduce the cross-interference in multi-UAV aided FD-NOMA system. Particularly, all UNs are initially clustered into K clusters using k-means clustering in the first stage where each cluster is served by an UAV. Furthermore, each cluster is further divided into sub-clusters and each sub-clusters are operated in FD-NOMA scheme. Finally, to control interferences, a sum-rate throughput maximization problem is formulated for each UAV to jointly optimize uplink and downlink power allocation and UAV placement. The joint optimization problem is non-convex and difficult to solve directly, for which we decoupled the original problem by addressing UAV placement and power allocation separately. We first fix the UAV position and then solve the problem iteratively using successive convex approximation (SCA) method. By utilizing brute-force search algorithm, an optimal UAV placement is later performed which corresponds to maximum possible sum-rate throughput. Simulation results demonstrate that the proposed solution for the considered FD-NOMA system outperforms the conventional schemes.**

***Index Terms*— Unmanned aerial vehicles (UAVs), full-duplex (FD), non-orthogonal multiple access (NOMA), optimal UAV placement, power allocation, sum-rate maximization.**

Manuscript received March 23, 2021; revised July 11, 2021; accepted September 12, 2021. Date of publication September 24, 2021; date of current version April 11, 2022. This work was supported by the Ministry of Science and Technology of Taiwan under Grant MOST 109-2221-E-110-050-MY3 and Grant MOST 110-2221-E-110-020. The associate editor coordinating the review of this article and approving it for publication was X. Wang. *(Corresponding author: Keshav Singh.)*

Mayur Katwe, Keshav Singh, and Chih-Peng Li are with the Institute of Communications Engineering, National Sun Yat-sen University, Kaohsiung 80424, Taiwan (e-mail: mayurkatwe@gmail.com; keshav.singh@mail.nsysu.edu.tw; cpli@faculty.nsysu.edu.tw).

Prabhat Kumar Sharma is with the Department of ECE, Visvesvaraya National Institute of Technology, Nagpur, Maharashtra 440010, India (e-mail: prabhatsharma@ece.vnit.ac.in).

Zhiguo Ding is with the Department of Electrical and Electronic Engineering, The University of Manchester, Manchester M13 9PL, U.K. (e-mail: zhiguo.ding@manchester.ac.uk).

Color versions of one or more figures in this article are available at https://doi.org/10.1109/TWC.2021.3113640.

Digital Object Identifier 10.1109/TWC.2021.3113640

I. Introduction

OWING to their high mobility and flexibility, the developments in unmanned aerial vehicles (UAVs) have gained growing attention in recent years for various applications of fifth generation and beyond (B5G) wireless networks such as rescue operations, support and surveillance, packet delivery, cellular data offloading and dissemination, etc [1]–[5]. The utilization of UAVs as flying base stations or mobile relays provide an eminent solution to the critical issues of the existing cellular networks which include coverage capability, high data traffic and massive user nodes (UNs) connectivity [4]–[10]. The explosive growth of mobile devices and ever increasing demand of high data rates are the critical challenges in B5G networks which involves high quality video and ultra-high data streaming [3]–[5]. In addition to traffic volume, the power constrained mobile devices and bandwidth limited wireless channels have impelled the inevitable search of high spectrum and power efficient wireless communication systems [8]–[12]. The advent of full-duplex (FD) communication and non-orthogonal multiple access (NOMA) schemes have emerged as promising technologies in recent years which are capable to provide higher rate throughput along with improved spectral efficiency [7]–[15]. Unlike conventional orthogonal multiple access (OMA) scheme based time and frequency multiplexing, the NOMA serves multiple UNs on same time-frequency allocations by exploiting power multiplexing which provide higher rate throughput, low latency communication and improved spectral efficiency [16].

The UAV aided FD-NOMA schemes are especially advantageous in ultra-low latency networks, poor channel conditions and high coverage areas [17], [18]. In such scenarios, FD-NOMA provides excellent user fairness and ensures efficient spectrum utilization while, multiple UAV deployment provides flexible configuration [12]. However, the inevitable cross-interference in up-link (UL) and down-link (DL) transmission such as strong self-interference (SI) and co-channel interference (CCI), respectively, are prime bottlenecks in FD-NOMA scheme [11]. Particularly, SI arises due to reception of signal through own transmitting antenna whereas CCI occurs at DL UNs due to simultaneous up-link transmission (UL). The problem of cross-link interference is trivial for OMA scheme, however, it becomes more severe for

FD-NOMA as UN density increases [19]. Besides, the channel conditions are subject to vary due to UAV position in UAV aided communication and hence the UAV placement becomes major concern in the performance of UAV aided communication network [20], [21].

In general, the power domain NOMA system employs successive interference cancellation (SIC) at receivers which exploits the channel differences of the UNs. The performance of NOMA systems depends upon favorable SIC at UNs which although dependent upon user pairing or user clustering schemes [18], [22], [23]. The NOMA system becomes extremely complicated with increase in UN density as the computational complexity of SIC techniques increases [24]. The UNs clustering schemes targets to reduce SIC complexity and even cross-interference upto possible extent by grouping the network into smaller NOMA clusters which reduces and ensures maximum sum-rate throughput for whole system. Hence, investigation on the dynamic user clustering schemes are equally mandatory for successful implementation of FD-NOMA schemes.

A. Related Works

There have been growing research efforts for UAV-assisted communication including single to multiple UAV deployment. Most commonly applications of UAV enabled communication are UAV as a flying base station [6], [9], [10], [25]–[28] and UAV as a mobile relay [8], [17], [29], [30]. The major investigations in the existing works have targeted to improve UAV services in terms of rate throughput [17], [25], data traffic [26], [29], power control [27], [30], coverage capability [6], [9], [10], energy and spectral efficiency [28], UAV trajectory design [19], cooperating base-stations and beamforming design [8]. Among all these topics, UAV deployment for enhancing rate-throughput and coverage capability under low transmit power are of immense interest [9], [10], [20], [27], [31], [32]. Particularly, the authors in [25] have introduced UAVs as a solution for deploying dense networks by considering them as flying base stations (BSs) and obtained the optimal position of UAVs and associating users in order to maximize user satisfaction with provided data rates. In [26], a new hybrid network architecture have been proposed where an UAV is employed as an flying BS to offload data for cell edge users by flying cyclically along the cell edge. The problem of 3-D placement of an UAV and transmit power allocation for UL and DL operations in the network with coexisting BSs have been investigated in [27]. In [10] and [9], the authors have investigated deployment of UAV for small cells for the optimal UAV altitude determination under maximum coverage and minimum required transmit power, respectively. In [6], the problem of minimizing average euclidean distance between UAV-UNs has been formulated. The UAV deployment, user clustering, and band allocation have been optimized in [28] to minimize the number of required UAVs and to improve the coverage rate of the users. The authors in [29] have investigated the outage probability, throughput and coverage probability of UAV selection strategies based on best harmonic mean (HM) and best DL signal to noise ratio (SNR). In [30], joint 3-D location and power optimization for UAV as a relay have been investigated to maximize sum-rate of all UNs subject to constraints of line of sight (LOS) connectivity between UN and UAV. A problem of joint UAV trajectory and power control for maximizing sum-rate throughput in multi-UAV interference coordination framework with same time and frequency allocation has been formulated in [19].

Earlier mentioned works in [6], [8]–[10], [17], [19], [25]–[30] have considered resource allocation either on different time allocation or frequency allocation which gain limited spectral efficiency. To further improve the spectral efficiency and quality-of-service (QoS), many research works have been recently carried out by integrating FD and NOMA schemes into UAV aided communication systems [14], [20], [21], [31]–[33]. To address spectrum scarcity, a multiple UAV aided FD-NOMA has been investigated in [14] and shown to achieve higher ergodic sum capacity and ergodic capacity gains when compared to HD. In [20], the problem of resource allocation for multi-small cell networks with FD UAVs as aerial BSs with imperfect SIC has been considered to maximize the sum-rate throughput. The UAV position and power allocation have been jointly optimized in [32] to improve the performance of the NOMA-UAV network. The authors in [21] have targeted to maximize DL sum-rate whilst guaranteeing a certain minimum requirement for UL transmission rate by jointly optimizing the transmission power and location. A FD based UAV relaying for multiple source-destination pairs has been investigated in [33] for maximizing rate-throughput with dynamic time-division multiple access (TDMA) based user-scheduling protocols.

Although, the rendered developments with NOMA and FD systems secure improved spectral efficiency, the issues of imperfect SIC, SI and CCI becomes too critical for highly dense FD-NOMA networks and hence degrade the overall performance of the system [11]–[13]. To overcome these practical constraints, few works [11], [18], [22]–[24], [34] have been investigated to reduce the effect of imperfect SIC and cross-interference through user association or user clustering techniques. These techniques generally relies on the perfect CSI or on the perfect UN location acquisition. Commonly, the user clustering methods involve game theory approach to maximize system performance such as energy and spectral efficiency [11], [18], [22], [24], [34] or improved outage probability and ergodic capacity [35]. Like, the authors in [11], [24] adopted game theory approach to assign user clustering which involved select and swap operations with partition forming. In [18], user based clustering and sum-rate maximization under optimal power allocation for UL and DL UNs have been studied based on channel gain differences among UNs in NOMA network. The authors in [18] have considered the cluster-size with two UNs only without guaranteeing spectral efficiency. A brute force search algorithm has been adopted in [34] for user clustering to maximize the overall spectral efficiency and user fairness subject to user-specific QoS and the total transmit power constraints. A distributed clustering scheme based on fractional error factor, clustering bandwidth and QoS constraint has been investigated in [23] for maximizing sum-rate throughput and user fairness.

The clustering techniques in [11], [24], [34] although have considered large cluster size, the cost of computationally complex is higher due to involved heuristic approaches and such techniques become difficult to cope with scalability. For a dynamic scenario, the authors in [22] have proposed an online unsupervised k-means clustering based algorithm for the optimal power allocation policy in NOMA systems.

B. Motivation and Contribution

As discussed above, the user clustering plays vital role in improving performance of FD-NOMA in terms of interference reduction. However, the problem related to user clustering (association) and resource allocation in multi-UAV assisted FD-NOMA systems have not been well researched. To the best of authors' knowledge, the combined exploitation of multiple UAV-aided communication in FD-NOMA with dynamic user clustering to improve coverage capability and QoS for UL and DL transmission has not been investigated yet, both from theoretic as well resource allocation perspective. Motivated by this background, in this paper, we consider a multi-UAV aided FD-NOMA cellular network where UAV serves as flying base-stations and investigate the problem of maximizing overall sum-rate throughput under UAV placement and the transmit power budget at each UL node and at UAV. Based on k-means clustering, we propose an unconventional two-stage clustering algorithm to effectively reduce CCI and SI and improve overall throughput of the system. The main contributions in this work are pointed as follows:

1) We consider a multiple UAV enabled FD-NOMA communication system in which each UAV operates under FD mode in order to assist multiple UL and DL UNs simultaneously with same time and frequency allocation, and all UNs operate in half-duplex (HD) mode.
2) In order to reduce the effects SI and CCI, an unconventional two-stage dynamic user clustering algorithm is proposed. In the first stage, all the UNs are clustered into group equal to the number of UAVs using unsupervised k-means algorithm. Later in the next stage, using elbow k-means method, each cluster is further divided into dynamic number of sub-cluster based on UNs' location and density. The UNs belonging to same sub-cluster operate in FD-NOMA fashion whereas the sub-clusters are operated under OMA schemes which results in significant reduction of SI and CCI and completely mitigates the inter UAV interference.
3) Next, we formulate a sum-rate throughput maximization problem for each cluster (or UAV) subject to transmit power budget at each UL node, the total power budget at UAV and UAV position. Due to inherent non-convexity of the original formulated problem, it becomes very difficult to find the optimal solution. Therefore, we decouple the original problem into two sub-problems which address UAV placement and power allocation separately. We first fix the UAV position and solve the power allocation problem iteratively using successive convex approximation (SCA) method. Later, through brute-force search (BFS) algorithm, the optimal UAV placement corresponding to maximum sum-rate throughput for the UNs is performed.
4) The computational complexity and numerical simulations are provided to demonstrate the effectiveness of the proposed solution. As a benchmark, we compare the performance of the proposed algorithm with optimal brute-force search (BFS) method and conventional HD-NOMA, single stage NOMA clustering (without sub-clustering) and OMA schemes subject to convergence, optimality, traffic conditions, power budget, network density, and self-interference cancellation capabilities. It is illustrated that the proposed power allocation algorithm converges within few iterations. The proposed solution involving SCA based power allocation and BFS for UAV placement is although slightly sub-optimal, however, it attains significantly reduced computational complexity when compared to the joint BFS algorithm.

C. Notations and Paper Structure

Notations: Throughout the paper, the scalar, vectors, matrices and sets are represented by regular, bold lowercase, bold uppercase and scripts, respectively. $|\mathcal{S}|$ represents cardinality of the set $\mathcal{S}$. $||\boldsymbol{l}||_2$ indicates the ℓ_2 norm of the vector $\boldsymbol{l}$. $p^{(a)}$ denotes value of parameter p at a^{th} iteration whereas $\{p_i\}$ indicates the accumulation of all variables $p_i, \forall i$. $n \sim \mathcal{CN}(\mu, \sigma^2)$ denotes that n is circularly symmetric Gaussian random variable with a mean of μ and variance σ^2.

Structure: The rest of the paper is organized as follows. Section II describes the adopted system model for the UAV aided FD NOMA scheme. In section III, we design a novel user dynamic clustering and present the problem of optimal power allocation and UAV placement to maximize sum-rate throughput in the network. Section IV addresses the solution of formulated optimization problem and discuss on its computational complexity. Section V describes the baseline OMA scheme. Simulations results based are presented and analyzed in Section VI and finally, Section VII concludes the work.

II. System Model: Multiple UAV-Aided Cellular System

Consider an example of multi-UAV assisted cellular network[1] with randomly distributed N UNs and K UAVs as shown in Fig. 1. Assuming that the true position of all UNs is known and defined as $\boldsymbol{n}_i = [n_{x_i}, n_{y_i}, 0]^T \in \mathbb{R}^3, \forall i \in \boldsymbol{\mathcal{N}}$ (for $\boldsymbol{\mathcal{N}} = \{1, \ldots, N\}$). In the given network, the ground UNs dynamically behave as up-link (UL) or down-link (DL) users and K UAVs, which work as flying base-stations, are utilized to serve them. Let there exists I UL UNs and J DL UNs in the given network at a particular instant. The set of all UL UNs, DL UNs and UAVs are collectively defined as $\boldsymbol{\mathcal{I}} = \{1, \ldots, I\}$, $\boldsymbol{\mathcal{J}} = \{1, \ldots, J\}$ and $\boldsymbol{\mathcal{K}} = \{1, \ldots, K\}$, respectively.

[1]A single UAV system can be although considered, however, the multi-UAV system gain better coverage capability and improved sum-rate throughput when compared to the single UAV system [9], [10], [17]. The multi-UAV systems particularly provide flexible and on-demand service by maintaining optimal fairness for all the UNs especially in large scale network.

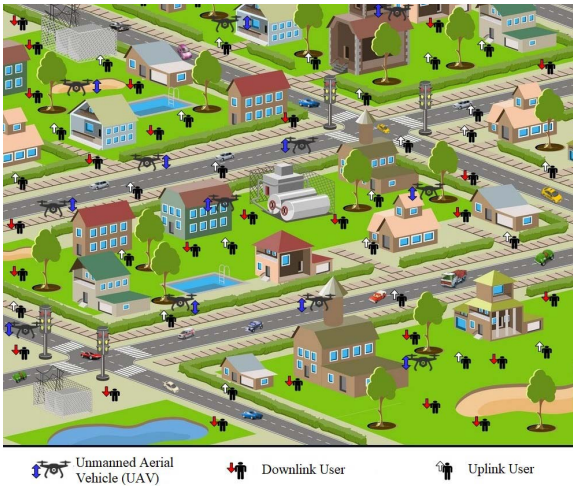

Fig. 1. An Example of Multiple UAV based Cellular Network.

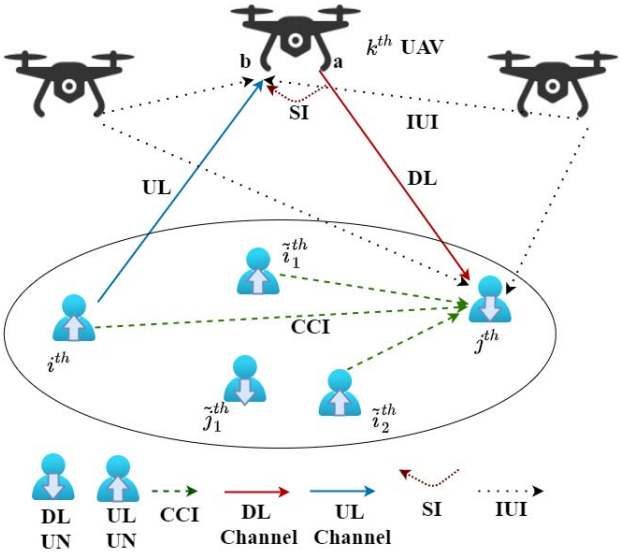

Fig. 2. An illustration of single NOMA cluster.

Each UAV operates in FD mode and therefore has two antennas i.e., one for transmitting the signals to the DL UNs and second one for receiving the signals from the UL users simultaneously. In addition, we also assume that all the UNs are equipped with a single antenna and operate in half duplex mode.

A. Channel Model

For accountability of practical communication environment, the UN-UAV i.e., ground-air links are modeled as line of sight (LOS) with probability, P. However, the air-air and ground-ground links are modeled as LOS and non-line of sight (NLOS), respectively as in [30], [31]. Additionally, the link between transmitting and receiving antenna of UAV is considered as LOS. The path identification i.e., either LOS or NLOS paths for all possible UN-UAV and UN-UN links are known to the network as a prior information.

Denote g_{ik}^{u} as the channel gain between i^{th} UL UN and k^{th} UAV, g_{kj}^{d} as the channel gain between j^{th} DL UN and k^{th} UAV, g_{ij}^{n} as channel gain between i^{th} and j^{th} UNs, g_{k}^{a} as channel gain between transmitting antenna and receiving antenna of k^{th} UAV and $g_{k\widetilde{k}}$ as channel gain between k^{th} and $\widetilde{k}^{th}$ UAV. Hence, the channel gains are given as

$$g_{ik}^{u} = \begin{cases} \alpha_L \left(d_{ik}^{u}\right)^{-\gamma}, & \text{with } P, \\ \alpha_N \left(d_{ik}^{u},\right)^{-\gamma}, & \text{with } 1-P, \end{cases} \tag{1}$$

$$g_{kj}^{d} = \begin{cases} \alpha_L \left(d_{kj}^{d}\right)^{-\gamma}, & \text{with } P, \\ \alpha_N \left(d_{kj}^{d},\right)^{-\gamma}, & \text{with } 1-P, \end{cases} \tag{2}$$

$$g_{ij}^{n} = \alpha_N \left(d_{ij}^{n}\right)^{-\gamma}, \tag{3}$$

$$g_{k}^{a} = \alpha_L \left(d_{k}^{a}\right)^{-\gamma}, \tag{4}$$

$$g_{k\widetilde{k}} = \alpha_L \left(d_{k\widetilde{k}}^{a}\right)^{-\gamma}, \tag{5}$$

where $P = \frac{1}{1+\zeta \exp(-\beta(\theta-\zeta))}$ is LOS probability of UN (i^{th} UL or j^{th} DL) to the k^{th} UAV link, θ (θ_{ik}^{u} or θ_{kj}^{d}) is the elevation angle between the UN and UAV, ζ and β are environment dependent values, α_L and α_N are attenuation coefficient for LOS and NLOS channels, respectively. Moreover, $d_{ik}^{u}, d_{kj}^{d}, d_{ij}^{n}, d_{k}^{a}$ and $d_{k\widetilde{k}}$ denote the distances between i^{th} UL UN and k^{th} UAV, j^{th} DL UN and k^{th} UAV, i^{th} and j^{th} UNs, and k^{th} UAV and $\widetilde{k}^{th}$ UAV, respectively. γ represents the path loss exponent. Since we adopted low altitude profile for the UAVs placement ($20\text{m} \leq h \leq 100\text{m}$), the considered LOS probability which is modelled as simple modified Sigmoid function (S-curve) suits the real environment [36]. The parameters ζ and β are S-curve parameters which are environment dependent and can be obtained or set using pilot signals and initial calibrations [37].

B. Signal Model

Assuming that all UL UNs, DL UNs and the UAVs operates in a single NOMA cluster i.e., under same time and frequency allocation. Due to which the intended UL and DL transmission to and from UAV experiences various interferences from the other UNs and UAVs as illustrated in Fig. 2. The i^{th} UL UN and j^{th} DL UN while communicating with k^{th} UAV experiences inter-node interference (INI) from the other UL UNs and DL UNs, respectively. Moreover, the DL signal transmission from other UAVs also interfere the desired signal which is referred as inter UAV interference (IUI). Due to the adoption of FD scheme, there exist cross interferences i.e., SI and CCI in UL and DL transmission from all the DL and UL UNs, respectively. Particularly, the SI arises due to the reception of signal through own transmitting antenna whereas CCI occurs at DL UNs due to the simultaneous UL transmission.

Let P_k denotes the total transmission power of k^{th} UAV and p_{kj}^{d} and s_{kj}^{d} be the power allocated and intended symbol transmitted by k^{th} UAV for j^{th} DL UN, respectively, such that $\mathbb{E}\left[|s_{kj}^{d}|^2\right] = 1, j \in \mathcal{J}$. Then, the transmitted signal by

k^{th} UAV is given as

$$x_k^d = \sum\nolimits_{j=1}^{J} \sqrt{p_{kj}^d} s_{kj}^d \,. \tag{6}$$

Similarly, let s_i^u be the symbol transmitted by i^{th} UL UN with power p_i^u such that $\mathbb{E}\left[|s_i^u|^2\right] = 1, i \in \boldsymbol{\mathcal{I}}$. Then, the transmitted signal by i^{th} UL UN is given by

$$x_i^u = \sqrt{p_i^u} s_i^u \,. \tag{7}$$

Now, the received signal received by k^{th} UAV from i^{th} UL UN can be given as

$$\begin{aligned} y_{ik}^u = & \underbrace{g_{ik}^u x_i^u}_{\text{Desired signal}} + \underbrace{\sum\nolimits_{\widetilde{i} \in \boldsymbol{\mathcal{I}}/\{i\}} g_{\widetilde{i}k}^u \sqrt{p_{\widetilde{i}}^u} s_{\widetilde{i}}^u}_{\text{INI}} + \underbrace{g_k^a x_k^d}_{\text{SI}} \\ & + \underbrace{\sum\nolimits_{\widetilde{k} \in \boldsymbol{\mathcal{K}}/\{k\}} g_{k\widetilde{k}} x_{\widetilde{k}}^d}_{\text{IUI}} + \underbrace{n_k}_{\text{Noise}} . \end{aligned} \tag{8}$$

And, the signal received by j^{th} DL UN from k^{th} UAV can be expressed as

$$\begin{aligned} y_{kj}^d = & \underbrace{g_{kj}^d \sqrt{p_{kj}^d} s_{kj}^d}_{\text{Desired Signal}} + \underbrace{\sum\nolimits_{\widetilde{j} \in \boldsymbol{\mathcal{J}}/\{j\}} g_{kj}^d \sqrt{p_{k\widetilde{j}}^d} s_{k\widetilde{j}}^d}_{\text{INI}} + \underbrace{\sum\nolimits_{i \in \boldsymbol{\mathcal{I}}} g_{ij}^n x_i^u}_{\text{CCI}} \\ & + \underbrace{\sum\nolimits_{\widetilde{k} \in \boldsymbol{\mathcal{K}}/\{k\}} g_{k\widetilde{k}} x_{\widetilde{k}}^d}_{\text{IUI}} + \underbrace{n_j^d}_{\text{Noise}} . \end{aligned} \tag{9}$$

In the above equations (8) and (9), g_{ik}^u represent UL channel between i^{th} UL UN and k^{th} UAV, g_{kj}^d represent UL channel between j^{th} DL UN and k^{th} UAV, g_{ij}^n represent CCI channel between i^{th} UL UN and j^{th} DL UN, $g_{k\widetilde{k}}$ represent IUI channel between k^{th} and $\widetilde{k}^{th}$ UAVs and g_k^a represent SI channel in k^{th} UAV. $n_k \sim \mathcal{CN}(0, \sigma_k^2)$ and $n_j^d \sim \mathcal{CN}(0, \sigma_j^2)$ are the zero-mean Gaussian noise at k^{th} UAV and j^{th} DL UN with variance of σ_k^2 and σ_j^2, respectively. For simplicity, we assume $\sigma^2 = \sigma_k^2 = \sigma_j^2$. Note that the total interference power dominates the performance of the UL and DL UNs. Therefore, we apply NOMA for UL UNs and at each UAV for DL UNs along with user clustering.

In the given network, the NOMA model performs user ordering based on channel gain such that UN with low channel gain is weakest and UN with high channel gain is strongest [11], [16]. In other words, the sets of UL and DL UNs are arranged in ascending order of their channel gain. Later, the receiver performs SIC to mitigate INI from strong users. After SIC, the rate throughput of strong users is not subject to INI, instead, it depends on its power allocation and channel gain. However, the rate throughput for weak users depend more upon the INI from other strong users and therefore it becomes very critical for low order users especially when there exists large number of UNs. Besides, it also becomes impractical to implement the single centralized NOMA model for high UN density network due to high complexity of performing SIC techniques [22], [23]. Furthermore, the CCI dominates the performance of the DL UNs [11]. Particularly, the IUI becomes more significant in the received signal with large number of UAVs. Overall, the interference in the received signal become highly dominant than desired signal which results into very poor UL and DL signal to noise ratio (SNR). Therefore, in this paper, we investigate a dynamic user clustering algorithm to effectively mitigate the interferences.

Remark 1: The implementation of SI cancellation techniques can possibly mitigate their effects, however, there still exist residual self-interference (RSI) which can be considered as hardware impairment.

The SI signals are a function of a known transmitted signal and thus can be cancelled. The pilot signal of FD node can be echoed back to itself and moreover, the received echo signal have high signal strength due to which the SI can be estimated with high accuracy. Moreover, the effective SI suppression can be achieved using analog and digital SI cancellation techniques [11]. However, there still remains some part for SI due to hardware impairments such as transmitter and distortion which is termed as RSI [38]. We assume that an efficient SI cancellation techniques based on digital SI cancellation techniques is already employed.[2] We denote RSI coefficient τ as the hardware impairment which quantify the SI cancellation capability. We discuss the performance analysis of the proposed solution for wide range of RSI coefficient values (10^{-12} to 10^{-6}) shortly in the paper.

C. CSI Estimation and SIC Cancellation

CSI Estimation: It is assumed that the UAVs performs perfect CSI acquisition as in [7], [9], [24], [27]. The CSI estimation can be performed at the UAV by exploiting the channel reciprocity between forward and backward transmissions through orthogonal pilot signals. The CSI estimation may not be perfect in time-varying environment due to the combined influence of path loss, channel fading and power attenuation. However, for sufficiently long training sequence, it is proved that the effect of CSI error is negotiable. The considered assumption of perfect CSI estimation suits for block fading channels where channels are nearly static within particular time-frequency coherence block and long training sequences [11].

SIC Cancellation: It is worth pointing that the perfect SIC in the proposed FD-NOMA system is taken into account in this paper as considered in [11], [24]. However, in practical scenarios, the assumption of perfect SIC at the receiver might not be ideal due to error propagation and complexity scaling [39]. The NOMA systems have potential to achieve higher spectral efficiency under perfect SIC. For sake of simplicity in performance evaluation of the proposed theoretical model, the consideration of imperfect SIC is compromised. The results of the proposed FD-NOMA can be treated as theoretical guidelines for impact of RSI and CCI in FD-NOMA systems when nearly perfect SIC is achieved. The interested readers are advised to referred to [39] for more details on the effective SIC.

[2]If no SI mitigation technology is utilized, the considered system may not work.

III. Dynamic User Clustering, Hybrid NOMA and Problem Formulation

In this section, an unconventional two-stage user clustering algorithm is proposed which targets to reduce the interference level. Later, we formulate a sum-rate maximization problem subject to transmit power budget at each UL UN and at UAV and UAV position.

A. User Clustering and Ordering

In order to improve the performance of the described network model, we propose a multi-cluster NOMA system in spite of single NOMA cluster. The proposed clustering considers two-stage dynamic clustering which only depend upon the UNs location density (or UNs distribution) in the system and does not depend on the available CSI. In the first stage, all the UNs in the network are divided into K clusters. While in the second stage, the UNs belonging to the given cluster is further divided into sub-clusters where the number of sub-clusters are dynamically but optimally (as low as possible) selected. Particularly, we consider a hybrid multiplexing (called hybrid NOMA) scheme, i.e., NOMA is applied in each cluster and the users of different clusters receive signals via conventional OMA scheme. The primary motivation of the proposed two-stage clustering algorithm is to possibly reduce the interference level and achieve better UL and DL performance.

In first stage, we group all UNs into K different clusters using k-means based machine-learning algorithm which involves finding K optimal clusters and assigning individual UAV to each cluster. Assuming that the location of ground UNs is known as priory, we initially choose K random centroids and later each UN is assigned to the closest centroid. The collection of all UN belonging to same centroid forms a unique cluster. The centroid of each cluster is updated after UN-cluster assignment. We repeat the assignment and update the centroids until the clusters formulation remains same. Let $\boldsymbol{\phi} = \{\boldsymbol{\phi}_k, k \in \boldsymbol{\mathcal{K}}\}$ denotes the set of K cluster sets. Now, each cluster is assisted with an individual UAV and allows to operates under different frequency band. Let each cluster operates for different time/frequency allocation. This significantly eliminates the major interference factor, IUI from the received signal and also reduce INI upto some extent.

To further reduce INI, in second stage of clustering, each k^{th} cluster formed is dynamically sub-clustered into T_k sub-clusters using elbow k-means method. The basic idea behind this dynamic sub-clustering is to group the UNs of a clusters into T_K sub-clusters where the optimal value of T_k is determined based on UN density and their spatial distribution in that cluster. Particularly, in elbow k-means, we again exhibit k-means algorithm in each cluster for varying (increasing) value of T_k. For each value of T_k, the mean square distance (MSD) of UNs from their respective sub-clusters centroid is calculated and the least value of T_k is selected. Defining ϵ_c as the convergence parameter of MSD. Finally, T_k sets of sub-clusters i.e., $\boldsymbol{\phi}_{kt}, t \in \{1, \ldots, T_k\}$ for each k^{th} cluster are obtained. The bandwidth allocated to the k^{th} cluster is equally sub-divided into T_k sub-channels.

Algorithm 1 Dynamic User Clustering for Hybrid NOMA Scheme

Level 1: User Clustering

Input: Locations of UNs $\boldsymbol{n}_i, i \in \mathcal{N}$ and Number of clusters K
Perform **K-means** $(\{\boldsymbol{n}_i\}, K)$
Output: Clusters set, $\boldsymbol{\phi}_k, k = \mathcal{K} = \{1, \ldots, K\}$
if $|\boldsymbol{\phi}_k| > N_k^{\max}, \forall k \in \mathcal{K}$ **then** Repeat **K-means**
end if

Level 2: Dynamic Sub-clustering

Input: Clusters set $\boldsymbol{\phi}_k, \forall k \in \boldsymbol{\mathcal{K}}$
for $k \in \mathcal{K}$ **do**
  Initialize: $\text{MSD}^{(0)} = 0, t = 1$
  while $\text{MSD}^{(t)} - \text{MSD}^{(t-1)} < \epsilon_c$ **do**
    Perform **K-means** $(\boldsymbol{\phi}_k, t)$ and Obtain Subclusters, $\{\boldsymbol{\phi}_{kj}\}$ and Sub-centeriod, $\{\boldsymbol{c}_{kj}\}$
    $\text{MSD}^{(t-1)} = \frac{1}{t}\sum_{j=1}^{t} \frac{1}{|\boldsymbol{\phi}_{kj}|} \sum_{n=1}^{|\boldsymbol{\phi}_{kj}|} ||\boldsymbol{c}_{kj} - \boldsymbol{\phi}_{kj[n]}||^2$
    $t = t + 1$
  end while
  $T_k = t$
end for
Output: Sub-clusters, $\boldsymbol{\phi}_{kt}, \forall k \in \boldsymbol{\mathcal{K}}, \forall t \in \{1, \ldots, T_k\}$

Function: K-means $(\{\boldsymbol{p}_i\}, K)$

Input: 2-D data points, $\boldsymbol{p}_i$, Number of Clusters, K
Initialize: Randomly select K 2-D clusters center, $\{\boldsymbol{c}_k\}^{(0)}, a = 0$ and empty cluster sets $\boldsymbol{\phi}_k^{(0)} = \{\}, k \in \boldsymbol{\mathcal{K}}$
while $\{\boldsymbol{c}_k\}^{(a+1)} \neq \{\boldsymbol{c}_k\}^{(a)}$ **do**
  Calculate the distance between each UN and cluster centers, $d_{ik} = ||\boldsymbol{c}_k^{(a)} - \boldsymbol{p}_i||_2$
  Assign the UN to that cluster such that $\boldsymbol{\phi}_k^{(a+1)} = \{i | k = \min_k\{d_{i1}, \ldots, d_{ik}, \ldots, d_{iK}\}\}$
  Recalulate the cluster center, $\boldsymbol{c}_k^{(a+1)} = \frac{1}{|\boldsymbol{\phi}_k^{(a+1)}|}\sum_{j=1}^{|\boldsymbol{\phi}_k^{(a+1)}|} \boldsymbol{p}_j, j \in \boldsymbol{\phi}_k^{(a+1)}, \forall k \in \boldsymbol{\mathcal{K}}$
  $a = a + 1$
end while
Output: K clusters set and their centroids, $\boldsymbol{c}_k^{(a+1)}, \boldsymbol{\phi}_k^{(a+1)}, \forall k \in \boldsymbol{\mathcal{K}}$

Algorithm 1 summarizes the proposed dynamic user clustering procedure.

The expressions in (8) and (9) after dynamic user clustering can be respectively rewritten as

$$y_{ik,t}^u = g_{ik}^u \sqrt{p_{ik,t}^u} s_i^u + \sum\nolimits_{\tilde{i} \in \boldsymbol{\mathcal{I}_{kt}}/\{i\}} g_{\tilde{i}k}^u \sqrt{p_{ik,t}^u} s_{\tilde{i}}^u + g_k^a \sum\nolimits_{j \in \boldsymbol{\mathcal{J}}_{kt}} \sqrt{p_{kj,t}^d} s_{kj}^d + \bar{n}_k \,, \tag{10}$$

$$y_{kj,t}^d = g_{kj}^d \sqrt{p_{kj,t}^d} s_{kj}^d + \sum\nolimits_{\tilde{j} \in \boldsymbol{\mathcal{J}}_{kt}/\{j\}} g_{kj}^d \sqrt{p_{k\tilde{j},t}^d} s_{k\tilde{j}}^d + \sum\nolimits_{i \in \boldsymbol{\mathcal{I}}_{kt}} g_{ij}^n \sqrt{p_{ik,t}^u} s_i^u + \bar{n}_j^d \,, \tag{11}$$

where $i \in \boldsymbol{\mathcal{I}}_{kt}, j \in \boldsymbol{\mathcal{J}}_{kt}, k \in \boldsymbol{\mathcal{K}}$, $y_{ik,t}^u$ and $y_{jk,t}^d$ are the received signal at k^{th} UAV and j^{th} DL UN from i^{th} UL UN and k^{th} UAV with allocated power $p_{ik,t}^u$ and $p_{kj,t}^d$, respectively. Here, $\boldsymbol{\mathcal{I}}_{kt}$ and $\boldsymbol{\mathcal{J}}_{kt}$ denote the set of UL UNs and DL UNs belonging to the t^{th} sub-cluster set, $\boldsymbol{\phi}_{kt}$, respectively,

such that $\phi_{kt} = \mathcal{I}_{kt} \cup \mathcal{J}_{kt}$ and $\bar{n}_j^d \sim \mathcal{CN}(0, \sigma^2/T_k)$ and $\bar{n}_k \sim \mathcal{CN}(0, \sigma^2/T_k)$.

For each cluster or sub cluster, there should exist atleast one UL UN or/and DL UN. However, the increase in UNs in the network increases the cluster density for fixed UAVs. Due to the proposed second stage dynamic k-means (elbow k-means) method, optimal number of sub-clusters are selected even if UN density in a particular cluster increases. This increases the UN density in a sub-cluster too. Specifically, each sub-cluster is allocated with different frequency band which is sub-part of the frequency band allocated to the cluster. Since, the second stage optimally select the number of clusters, the frequency resource constraint does not affect the performance too significantly. Instead, the increased in UNs density in the sub-cluster increases the effect of RSI and CCI. This effect may be dominated if the number of UNs increases beyond certain threshold and their effective mitigation require increased power allocation. The power constraint and QoS constraint may lead to infeasible solution which should be avoided. For a given dynamic scenario, it is hard to obtain an analytical criterion or expression for the maximum allowed UNs in the cluster. We consider $N_k^{\max}$ as the maximum number of maximum number of UNs allowed in the cluster which can be set using select and execute operation through initial calibration or simulations.

B. User Ordering and Problem Formulation

We employ a hybrid scheme in which all the UAVs (or clusters) operates with independent time/frequency slot i.e., all UAVs operates in OMA fashion. Assuming that each UAV is assigned with unity bandwidth. Now, the unity bandwidth allocated to the k^{th} UAV is equally divided into the number of sub-clusters i.e., T_k sub-channels where each sub-clusters is allocated with for independent sub-frequency slots. However, the UNs belonging to same sub-clusters are allowed to operate in FD-NOMA fashion where they share same time and frequency slot. The multi-UAV placement and power allocation for whole system is extremely hard to achieve in centralized fashion (at any UAV) due to its higher computational complexity [40], moreover, it rapidly increases with UN density. Hence, in our proposed work, we considered that the power allocation UNs belonging to the particular cluster and a UAV placement for that cluster are performed in distributed fashion [41].

For the DL transmission, NOMA employs SIC at each DL UN based on UN ordering in the sub-cluster. Similarly, for the UL, the respective UAV of the sub-cluster employs SIC for the each UL UN. The UNs are arranged with ascending order of their channel gain and are assigned with increasing number of indexes such that first element corresponds to the weakest UN whereas the last element is the strongest user in sub-cluster set. In DL NOMA, the user j decode the signal of weak user $\widetilde{j}$ such that $\widetilde{j} < j$ in the sub-cluster whereas the signal of strong user j cannot be decoded by weak user $\widetilde{j}$ and hence, it becomes the INI for $\widetilde{j}^{th}$ user and similarly, it is also valid for UL transmission. The UL and DL transmission belonging to each sub-clusters experience RSI and CCI, respectively as

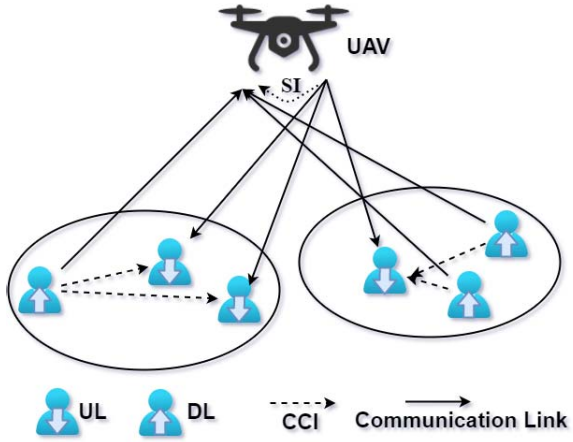

Fig. 3. UL and DL transmission after dynamic user clustering.

shown in Fig. 3. Since the UAV knows the interfering signal x_k^d and thus $g_k^a \sum_{j=1}^{J} x_k^d$ can be cancelled.

Considering that there exist $I_{kt} = |\mathcal{I}_{kt}|$ UL and $J_{kt} = |\mathcal{J}_{kt}|$ DL UNs in given t^{th} sub-cluster of k^{th} cluster. After optimal SIC decoding, the SINR related to i^{th} UL UN and j^{th} DL UN belonging to t^{th} sub-cluster of k^{th} cluster can be, respectively, given from (10) and (11) as

$$\gamma_{ik,t}^u = \frac{p_{ik,t}^u g_{ik}^u}{\sum_{c=i+1}^{I_{kt}} p_{ck,t}^u g_{ck}^u + \tau g_k^a \sum_{j=1}^{J_{kt}} p_{kj,t}^d + \frac{\sigma^2}{T_k}}, \tag{12}$$

$$\gamma_{kj,t}^d = \frac{p_{kj,t}^d g_{kj}^d}{\sum_{c=j+1}^{J_{kt}} p_{kc,t}^d g_{kj}^d + \sum_{i=1}^{I_{kt}} p_{ik,t}^u g_{ij}^n + \frac{\sigma^2}{T_k}}, \tag{13}$$

where τ denotes RSI coefficient. With consideration of unity bandwidth, the UL and DL rates for i^{th} UL and j^{th} DL UNs belonging to t^{th} sub-cluster of k^{th} UAV are, respectively, given as

$$R_{ik,t}^u = \frac{1}{T_k} \log_2 \left(1 + \gamma_{ik,t}^u\right), \tag{14}$$

$$R_{kj,t}^d = \frac{1}{T_k} \log_2 \left(1 + \gamma_{kj,t}^d\right). \tag{15}$$

The resource allocation scheme is implemented in distributed fashion where we aim to maximize the sum rate throughput through joint optimization of UL and DL power and UAV position at each UAV. Using (14) and (15), the primal power optimization for maximizing the sum-rate for UL and DL transmission is given as

$$\begin{aligned}
(\mathbf{P1}): \max_{\substack{\mathbf{u}_k, \{p_{ik,t}^u\} \\ \{p_{kj,t}^d\}}} \; & \left\{ \frac{1}{T_k} \sum_{t=1}^{T_k} \left\{ \sum_{i=1}^{I_{kt}} \log_2 \left(1 + \gamma_{ik,t}^u\right) \right.\right. \\
& \left.\left. + \sum_{j=1}^{J_{kt}} \log_2 \left(1 + \gamma_{kj,t}^d\right) \right\} \right\} \\
\text{s.t. } & \text{(C1): } p_{ik,t}^u \leq p^{u,\max}, i \in \mathcal{I}_{kt}, t \in \{1, \ldots, T_k\}, \\
& \text{(C2): } \sum_{t=1}^{T_k} \sum_{j \in \mathcal{J}_{kt}} p_{kj}^d \leq p^{d,\max}, \\
& \text{(C3): } \gamma_{ik,t}^u \geq \gamma^{u,\min}, i \in \mathcal{I}_{kt}, t \in \{1, \ldots, T_k\}, \\
& \text{(C4): } \gamma_{kj,t}^d \geq \gamma^{d,\min}, j \in \mathcal{J}_{kt}, t \in \{1, \ldots, T_k\}, \\
& \text{(C5): } \mathbf{u}^{\min} \leq \mathbf{u}_k \leq \mathbf{u}^{\max},
\end{aligned} \tag{16}$$

where (C1) and (C2) denotes that each UL UN transmission power is constrained by the maximum UL transmit power budget $p^{u,\max}$ and the total DL transmission power by a maximum DL transmit power budget $p^{d,\max}$, respectively. (C3) are (C4) corresponds to minimum QoS constraints where $\gamma^{u,\min}$ and $\gamma^{d,\min}$ denote the minimum rate requirements for UL and DL transmission, respectively, while constraint (C5) restricts the UAV position within a particular region. Along with the optimal power allocation, the performance of proposed framework also depends upon UAV position.

Remark 2: For guaranteeing the success of SIC, the signal strength gap among the UN should be considered.

Particularly, in DL NOMA case, the signal from the last user i.e., J_{kt}, in the sub-cluster receives no interference from other UNs $j < J_{kt}$ at UAV due to SIC. In other words,

$$\frac{p^d_{kJ_{kt},t} g^d_{kJ_{kt}}}{\sum_{i=1}^{I_{kt}} p^u_{ik,t} g^n_{iJ_{kt}} + \frac{\sigma^2}{T_k}} \geq \gamma^{d,\min} \tag{17}$$

Alternatively,

$$p^d_{kJ_{kt},t} \geq \frac{\eta^d_{kJ_{kt},t} \gamma^{d,\min}}{g^d_{kJ_{kt}}}, \tag{18}$$

where $\eta^d_{kJ_{kt},t} = \max\left(p^{u,\max} \sum_{i=1}^{I_{kt}} g^n_{iJ_{kt}}, \frac{\sigma^2}{T_k}\right)$. Let the above condition is satisfied by assigning minimum power to J_{kt} DL UN such that $p^d_{kJ_{kt},t} = \frac{\gamma^{d,\min}\eta^{d,\max}}{g^d_{kJ_{kt}}}$ where $\eta^{d,\max} = \max\left(\max\left(\boldsymbol{g}^n\right), \frac{\sigma^2}{T_k}\right)$ is the worst case interference which is defined for sake of simplicity in the derivation and $\boldsymbol{g}^n$ is the collection of the total CCI interference from all UL UNs for each j^{th} DL UN in the sub-cluster. Now, for the first and second penultimate DL UNs i.e., $J_{kt}-1$ and $J_{kt}-2$ the minimum power requirement can be expressed as

$$p^d_{k(J_{kt}-1),t} \geq \eta^{d,\max}\left\{\frac{\gamma^{d,\min}}{g^d_{k(J_{kt}-1)}} + \frac{\gamma^{d,\min 2}}{g^d_{kJ_{kt}}}\right\}, \tag{19}$$

$$p^d_{k(J_{kt}-2),t} \geq \eta^{d,\max}\left\{\frac{\gamma^{d,\min}}{g^d_{k(J_{kt}-2)}} + \gamma^{d,\min 2}\left\{\frac{\left(\gamma^{d,\min}+1\right)}{g^d_{kJ_{kt}}} + \frac{1}{g^d_{k(J_{kt}-1)}}\right\}\right\}, \tag{20}$$

respectively. Using induction, the minimum power requirement of any j^{th} DL UN under given rate constraint is obtained as

$$p^d_{kj,t} \geq \eta^{d,\max}\left\{\frac{\gamma^{d,\min}}{g^d_{kj}} + \gamma^{d,\min 2}\sum_{c=j+1}^{J_{kt}} \frac{\left(\gamma^{d,\min}+1\right)^{c-j-1}}{g^d_{kc}}\right\}, \tag{21}$$

where $j \in \boldsymbol{\mathcal{J}}_{kt}, t \in 1,\ldots,T_k$.

Similarly, for i^{th} UL UN, it can be proved that

$$p^u_{ik,t} \geq \frac{\eta^{u,\max}\gamma^{u,\min}\left(\gamma^{u,\min}+1\right)^{I_{kt}-i}}{g^u_{ik}}, \tag{22}$$

where $i \in \boldsymbol{\mathcal{I}}_{kt}, t \in \{1,\ldots,T_k\}, \eta^{u,\max} = \max\left(\tau g^a_k p^{d,\max}, \frac{\sigma^2}{T_k}\right)$ is the worst case interference. These above derived minimum power requirement expressions for all UL and DL UNs signifies the minimum power required for each UL and DL UNs to guarantee the success of SIC. So, the constraints (C3) and (C4) can be alternatively written as (22) and (21), respectively

Remark 3: The feasibility of problem (16) needs to be justified in terms of the constraints.

We discuss the feasibility of the original problem through two aspects: (a) the feasibility w.r.t power and QoS constraints and b) the feasibility w.r.t. power and UAV constraints

(a) Owing to the minimum SINR requirements and transmit power constraints, problem (**P1**) may be infeasible i.e., there may not exist feasible solution if the constraints are not well defined. For worst case scenario, let us consider only one sub-cluster in the given k^{th} cluster and define $I^{\max} = I_k, J^{\max} = J_k, g^{u,\min} = \min\left(\{g^u_{ik}\}\right)$ and $g^{d,\min} = \min\left(\{g^d_{kj}\}\right)$ as the maximum number of UL UN density and DL UN density and minimum UL and DL channel gain respectively. Using (17) and (18), the maximum UL power is lower bounded as

$$p^{u,\max} \geq \max\left(\{p^{u,\min}_{ik,t}\}\right) = \frac{\eta^{u,\max}\gamma^{u,\min}\left(\gamma^{u,\min}+1\right)^{I^{\max}-1}}{g^{u,\min}} \tag{23}$$

For DL case, the total DL power for UAV is lower bounded by the sum of the minimum power allocated for all DL UNs as $p^{d,\max} \geq \sum_{j=1}^{J_k} p^{\mathrm{d,min}}_{kj,t}$, where

$$\sum_{j=1}^{J_k} p^{\mathrm{d,min}}_{kj,t} = \sum_{j=1}^{J_k}\eta^{d,\max}\left\{\frac{\gamma^{d,\min}}{g^d_{kj}} + \gamma^{d,\min 2}\sum_{c=j+1}^{J_k}\frac{\left(\gamma^{d,\min}+1\right)^{c-j-1}}{g^d_{kc}}\right\} \tag{24}$$

$$\approx \frac{\eta^{d,\max}}{g^{d,\min}}\left\{J^{\max}\gamma^{d,\min} + \gamma^{d,\min 2}\sum_{c=1}^{J^{\max}}\left(\gamma^{d,\min}+1\right)^{c-1}\right\} \tag{25}$$

$$\approx \frac{\eta^{d,\max}\gamma^{d,\min}}{g^{d,\min}}\left\{J^{\max} + \left(\gamma^{d,\min}+1\right)^{J^{\max}} - 1\right\} \tag{26}$$

Hence, for feasibility of the problem (16), the maximum UL and DL power should be respectively lower bounded as

$$p^{u,\max} \geq \frac{\eta^{u,\max}\gamma^{u,\min}\left(\gamma^{u,\min}+1\right)^{I^{\max}-1}}{g^{u,\min}}, \tag{27}$$

$$p^{d,\max} \geq \frac{\eta^{d,\max}\gamma^{d,\min}}{g^{d,\min}}\left\{J^{\max} + \left(\gamma^{d,\min}+1\right)^{J^{\max}} - 1\right\}. \tag{28}$$

(b) Intuitively, the optimal power allocation vary with the channel gain condition and channel gain explicitly depend upon the UAV placement. Sometimes, the inappropriate

constraints for UAV position may lead to infeasible solution, especially when the optimal power allocation and the required rate throughput are constrained. Hence, both the constraints need to be determined. However, due to the strong coupling of power variables and UAV positions in both UL and DL SINR expressions ((12) and (13)), the formulation of analytical expression for the feasibility criterion for the given UAV and power allocation constraint is hard to obtain. Nevertheless, there exist other temporary ways to overcome this issue which include removing some bad environment users until the problems become feasible, gradually reducing the QoS level until the problems are feasible [42] or defining $\mathbf{u}^{\min}$ and $\mathbf{u}^{\max}$ using hit and trial methods.

The formulated joint optimization problem is non-convex in nature due to non-concavity of the objective function. It has been shown that such optimization problems are NP-hard [43]. Although, it is possible to find an optimal solution using exhaustive search methods, their implementation incurs high computational complexity overhead [43], [44]. Therefore, in practice, suboptimal but efficient algorithms are more preferred. In next section, we describe an efficient and low-complex algorithm to solve the joint optimization problem which first target to solve power allocation problem with fixed UAV position using SCA and later 3-D UAV placement is performed with given power allocation using BFS.

IV. Proposed Solution

Note that the objective function in (16) is non-convex due to coupling of variables. In addition, the non-convex problem (16) is difficult to transform into a convex one since the channel gain is dependent upon the UAV position. Therefore, the formulated problem is decoupled into a power allocation problem and UAV position optimization. More clearly, we solve the problem (16) in two stages. We first optimize UL and DL power allocation with UAV position[3] by developing new inner approximation based on an upper-bounding first order Taylor series approximation. Lastly, an exhaustive BFS is adopted to place the UAV at optimal position which corresponds to maximum sum-rate throughput.

A. Power Allocation Using SCA Method

With fixed UAV position as $\mathbf{u}_k = \mathbf{u}_o$, the problem of sum-rate maximization under optimal power allocation problem can be formulated into its equivalent epigraph form as

$$(\mathbf{P2}): \max_{\substack{\{r^u_{ik,t}\},\{p^u_{ik,t}\}\\ \{r^d_{kj,t}\},\{p^d_{kj,t}\}}} \left\{\sum_{t=1}^{T_k}\left\{\sum_{i=1}^{I_{kt}} r^u_{ik,t} + \sum_{j=1}^{J_{kt}} r^d_{kj,t}\right\}\right\}$$
$$\text{s.t. (C1) and (C2) of (}\mathbf{P1}\text{) and (21), (22),}$$
$$\text{(C6): } \log_2\left(1+\gamma^u_{ik,t}\right) \geq T_k r^u_{ik,t},$$
$$i \in \boldsymbol{\mathcal{I}}_{kt}, t \in 1,\ldots,T_k,$$
$$\text{(C7): } \log_2\left(1+\gamma^d_{kj,t}\right) \geq T_k r^d_{kj,t},$$
$$i \in \boldsymbol{\mathcal{I}}_{kt}, t \in 1,\ldots,T_k, \quad (29)$$

where the non-concave objective function in (**P1**) is equivalently transformed using slack variables, $\{r^u_{ik,t}\}$ and $\{r^d_{kj,t}\}$ which impose two extra constraints (C6) and (C7) and the QoS constraints (C3) and (C4) can be equivalently written as (22) and (21), respectively.

The optimization problem (29) is still non-convex owing to non-convex constraints (C6) and (C7). Particularly, (C6) and (C7) can be given as

$$\text{(C6): } \log_2\left(\frac{\sum_{c=i+1}^{I_{kt}} p^u_{ck,t}g^u_{ck} + \tau g^a_k \sum_{j=1}^{J_{kt}} p^d_{kj,t} + \frac{\sigma^2}{T_k} + p^u_{ik,t}g^u_{ik}}{\sum_{c=i+1}^{I_{kt}} p^u_{ck,t}g^u_{ck} + \tau g^a_k \sum_{j=1}^{J_{kt}} p^d_{kj,t} + \frac{\sigma^2}{T_k}}\right) \geq T_k r^u_{ik,t}, \quad (30)$$

$$\text{(C7): } \log_2\left(\frac{\sum_{c=j+1}^{J_{kt}} p^d_{kc,t}g^d_{kj} + \sum_{i=1}^{I_{kt}} p^u_{ik,t}g^n_{ij} + \frac{\sigma^2}{T_k} + p^d_{kj,t}g^d_{kj}}{\sum_{c=j+1}^{J_{kt}} p^d_{kc,t}g^d_{kj} + \sum_{i=1}^{I_{kt}} p^u_{ik,t}g^n_{ij} + \frac{\sigma^2}{T_k}}\right) \geq T_k r^d_{kj,t}, \quad (31)$$

which can further be rewritten as

$$\log_2\left(\sum_{c=i}^{I_{kt}} p^u_{ck,t}g^u_{ck} + \tau g^a_k \sum_{j=1}^{J_{kt}} p^d_{kj,t} + \frac{\sigma^2}{T_k}\right) - \log_2\left(\sum_{c=i+1}^{I_{kt}} p^u_{ck,t}g^u_{ck} + \tau g^a_k \sum_{j=1}^{J_{kt}} p^d_{kj,t} + \frac{\sigma^2}{T_k}\right) \geq T_k r^u_{ik,t}, \quad (32)$$

$$\log_2\left(\sum_{c=j}^{J_{kt}} p^d_{kc,t}g^d_{kj} + \sum_{i=1}^{I_{kt}} p^u_{ik,t}g^n_{ij} + \frac{\sigma^2}{T_k}\right) - \log_2\left(\sum_{c=j+1}^{J_{kt}} p^d_{kc,t}g^d_{kj} + \sum_{i=1}^{I_{kt}} p^u_{ik,t}g^n_{ij} + \frac{\sigma^2}{T_k}\right) \geq T_k r^d_{kj,t}, \quad (33)$$

respectively. However, the constraints (C6) and (C7) still remains non-convex. So, we adopt first order Taylor expansion to convert both constraints into equivalent convex form [45]. Let

$$\xi^u_{ik,t} \triangleq \log_2\left(\sum\nolimits_{c=i+1}^{I_{kt}} p^u_{ck,t}g^u_{ck} + \tau g^a_k \sum\nolimits_{j=1}^{J_{kt}} p^d_{kj,t} + \frac{\sigma^2}{T_k}\right), \quad (34)$$

$$\xi^d_{kj,t} \triangleq \log_2\left(\sum\nolimits_{c=j+1}^{J_{kt}} p^d_{kc,t}g^d_{kj} + \sum\nolimits_{i=1}^{I_{kt}} p^u_{ik,t}g^n_{ij} + \frac{\sigma^2}{T_k}\right). \quad (35)$$

The non-convexity of (C6) and (C7) is solved by SCA method which iteratively approximate $\xi^u_{ik,t}$ and $\xi^d_{kj,t}$ into its equivalent convex forms [27] using given power allocation from the previous iteration.

[3]Due to the mobility of the UAVs, the CSI vary dynamically and the precise high-speed CSI acquisition for each user sometimes become very difficult. Since the proposed FD-NOMA is based on the assumption of perfectly known CSI, the mobility of UAV may degrade the performance of the proposed solution involving fixed UAV placement. Hence, the mobility of UAV is compromised in the proposed work.

Let $\{p^u_{ik,t}\}^{(a-1)}$ and $\{p^d_{kj,t}\}^{(a-1)}$ denote the power allocation obtained at $(a-1)^{th}$ iteration which are used as given transmit power for a^{th} iteration. After each iteration, the following inequalities hold which provide convex upper bound of $\xi^u_{ik,t}$ and $\xi^d_{kj,t}$ as

$$\xi^u_{ik,t} \leq \hat{R}^{u^{(a)}}_{ik,t} \triangleq \left(\xi^{u}_{ik,t}{}^{(a-1)}\right) + \frac{\left(p^u_{ik,t} - p^{u}_{ik,t}{}^{(a-1)}\right) g^u_{ik}}{\log(2)\, 2^{\xi^{u(a-1)}_{ik,t}}}, \tag{36}$$

$$\xi^d_{kj,t} \leq \hat{R}^{d^{(a)}}_{kj,t} \triangleq \left(\xi^{d}_{kj,t}{}^{(a-1)}\right) + \frac{\left(p^d_{kj,t} - p^{d}_{kj,t}{}^{(a-1)}\right) g^d_{ik}}{\log(2)\, 2^{\xi^{d(a-1)}_{kj,t}}}, \tag{37}$$

respectively, where

$$\xi^{u^{(a-1)}}_{ik,t} = \log_2\left(\sum_{c=i+1}^{I_{kt}} p^{u^{(a-1)}}_{ck,t} g^u_{ck} + \tau g^a_k \sum_{j=1}^{J_{kt}} p^{d^{(a-1)}}_{kc,t} + \frac{\sigma^2}{T_k}\right), \tag{38}$$

$$\xi^{d^{(a-1)}}_{kj,t} = \log_2\left(\sum_{c=j+1}^{J_{kt}} p^{d^{(a-1)}}_{kc,t} g^d_{kj} + \sum_{i=1}^{I_{kt}} p^{u^{(a-1)}}_{ik,t} g^n_{ij} + \frac{\sigma^2}{T_k}\right). \tag{39}$$

Using the respective upper bound approximation of $\xi^u_{ik,t}$ and $\xi^d_{kj,t}$, the optimization problem (**P2**) can be rewritten into approximate form as

$$\textbf{(P3)}: \max_{\substack{\{r^u_{ik,t}\},\{p^u_{ik,t}\}\\ \{r^d_{kj,t}\},\{p^d_{kj,t}\}}} \left\{\sum_{t=1}^{T_k}\left\{\sum_{i=1}^{I_{kt}} r^u_{ik,t} + \sum_{j=1}^{J_{kt}} r^d_{kj,t}\right\}\right\}$$
$$\text{s.t. (C1) and (C2) of (P1) and (21), (22),}$$
$$(\widetilde{\text{C6}}), (\widetilde{\text{C7}}) \tag{40}$$

where the constraints $(\widetilde{\text{C6}})$ and $((\widetilde{\text{C7}}))$ are the concave approximation of the constraints (C6) and $((\text{C7})$ which are given as

$$(\widetilde{\text{C6}}): \log_2\left(\sum\nolimits_{c=i}^{I_{kt}} p^u_{ck,t} g^u_{ck} + \tau g^a_k \sum\nolimits_{j=1}^{J_{kt}} p^d_{kj,t} + \frac{\sigma^2}{T_k}\right) - \hat{R}^{u^{(a)}}_{ik,t} \geq T_k r^u_{ik,t},$$

$$(\widetilde{\text{C7}}): \log_2\left(\sum\nolimits_{c=j}^{J_{kt}} p^d_{kc,t} g^d_{kj} + \sum\nolimits_{i=1}^{I_{kt}} p^u_{ik,t} g^n_{ij} + \frac{\sigma^2}{T_k}\right) - \hat{R}^{d^{(a)}}_{kj,t} \geq T_k r^d_{kj,t}.$$

respectively. The objective function in the (**P3**) is affine, while the constraint (C1) and (C2) are linear. Since the left hand side (LHS) terms of constraints $(\widetilde{\text{C6}})$ and $(\widetilde{\text{C7}})$ in the problem (**P3**) are the logarithmic of affine functions which is concave, hence the constraints $(\widetilde{\text{C6}})$ and $(\widetilde{\text{C7}})$ are also convex. Therefore, the problem (**P3**) is convex in terms of variables $\{p^u_{ik,t}\}$ and $\{r^d_{kj,t}\}$ for given value of $\{r^u_{ik,t}\}$ and $\{r^d_{kj,t}\}$ and thus the solution can be obtained using standard convex optimization methods [45] or toolbox [46]. With given initial power allocation values, $\{p^u_{ik,t}\}^{(0)}$ and $\{p^d_{kj,t}\}^{(0)}$, the problem (**P3**) is iteratively solved at each UAV for maximum $L^{\max}$ iterations or until convergence for sum-rate,

Algorithm 2 Optimal Power Allocation for k^{th} UAV

1: **Input**: $\mathbf{u}_o$ and $L^{\max}$,
2: **Initialize**: $\mathbf{u}_k = \mathbf{u}_o$, $\{p^u_{ik,t}\}^{(0)} = p^{u,\max}$,$\{p^d_{kj,t}\}^{(0)} = \frac{p^{d,\max}}{\sum_{t=1}^{T_k} J_{kt}}$, $R^{(0)}_k = 0$ and $a = 0$
3: **while** $\frac{||R^{(a+1)}_k - ||R^{(a)}_k||}{||R^{(a)}_k||} \leq \epsilon_r$ or $a \leq L^{\max}$ **do**
4: a=a+1
5: Solve (40) with $\mathbf{u}_k = \mathbf{u}_o$ and calculate the sum rate $R^{(a)}_k$,
6: $R^{(a)}_k = \sum_{t=1}^{T_k}\left\{\sum_{i=1}^{I_{kt}} r^{u}_{ik,t}{}^{(a)} + \sum_{j=1}^{J_{kt}} r^{d}_{kj,t}{}^{(a)}\right\}$
7: **end while**
8: **Output**: $R_k = R^{(a)}_k$

$R_k = \sum_{t=1}^{T_k}\left(\sum_{i\in\mathcal{I}_{kt}} r^u_{ik} + \sum_{j\in\mathcal{J}_{kt}} r^d_{kj}\right)$ is achieved. Let ϵ_r denotes the convergence factor for the sum-rate. The proposed SCA method for achieving the *optimal power allocation*[4] for given UAV position, $\mathbf{u}_o$, is summarized in Algorithm 2.

Next, the convergence of the Algorithm 2 is guaranteed as follows:

Proposition 1: Given an initial feasible solution, the proposed SCA based power allocation method in Algorithm 2 converges to a stationary point satisfying the Karush-Kuhn-Tucker (KKT) conditions of original power allocation problem, (**P2**).

Proof: Let $\boldsymbol{p}^{u^{(a-1)}}_{k,t}$ be the set of power allocation for all the UL and DL UN in t^{th} cluster obtained at a^{th} SCA iteration which is utilized in next i.e., $(a+1)^{th}$ iteration. It can be shown that $\hat{R}^{u^{(a+1)}}_{ik,t} \leq \hat{R}^{u^{(a)}}_{ik,t}$ and $\hat{R}^{d^{(a+1)}}_{kj,t} \leq \hat{R}^{d^{(a)}}_{kj,t}$, and hence, $r^{d}_{kj,t}{}^{(a+1)} \geq r^{d}_{kj,t}{}^{(a)}$ and $r^{u}_{ik,t}{}^{(a+1)} \geq r^{u}_{ik,t}{}^{(a)}, \forall i \in \mathcal{I}_{kt}, \forall j \in \mathcal{J}_{kt}, \forall t \in \{1,\ldots,T_k\}$. This implies that the total sum-rate function R_k monotonically increases as a increases. Due to the power constraints, the R_k is bounded proposed and hence the Algorithm 2 converges. Following the results from [47], the proposed algorithm in this work based on SCA converges to a KKT point of the original power allocation problem (**P2**) if the following conditions are satisfied:

1) $\xi^u_{ik,t} \leq \hat{R}^{u^{(a)}}_{ik,t}$ and $\xi^d_{kj,t} \leq \hat{R}^{d^{(a)}}_{kj,t}$,
2) $\xi^{u^{(a-1)}}_{ik,t} = \hat{R}^{u^{(a)}}_{ik,t}\Big|_{\boldsymbol{p}^u_{k,t}=\boldsymbol{p}^{u^{(a-1)}}_{k,t}}$ and $\xi^{d^{(a-1)}}_{kj,t} = \hat{R}^{d^{(a)}}_{kj,t}\Big|_{\boldsymbol{p}^u_{k,t}=\boldsymbol{p}^{u^{(a-1)}}_{k,t}}$,
3) $\left.\frac{\partial \xi^u_{ik,t}}{\partial p^u_{ik}}\right|_{\boldsymbol{p}^u_{k,t}=\boldsymbol{p}^{u^{(a-1)}}_{k,t}} = \left.\frac{\partial \hat{R}^u_{ik,t}}{\partial p^u_{ik}}\right|_{\boldsymbol{p}^u_{k,t}=\boldsymbol{p}^{u^{(a-1)}}_{k,t}}$ and $\left.\frac{\partial \xi^d_{kj,t}}{\partial p^d_{kj}}\right|_{\boldsymbol{p}^u_{k,t}=\boldsymbol{p}^{u^{(a-1)}}_{k,t}} = \left.\frac{\partial \hat{R}^d_{kj,t}}{\partial p^d_{kj}}\right|_{\boldsymbol{p}^u_{k,t}=\boldsymbol{p}^{u^{(a-1)}}_{k,t}}$,

where $\forall i \in \mathcal{I}_{kt}, \forall j \in \mathcal{J}_{kt}, \forall t \in \{1,\ldots,T_k\}$ and Δ represent the gradient of the function. Since $\xi^u_{ik,t}$ and $\xi^d_{kj,t}$ are concave and differentiable for any power values, they are bounded above by their first-order Taylor approximation which validate

[4]*The optimization problem* (16) *is non-concave. Here, the optimal power allocation solution of the problem* (40) *is defined in a locally optimal sense and it is referred to as a local maximizer for the problem* (16).

the first condition. The second condition is straightforward to obtain by substituting $\boldsymbol{p}_{k,t}^{u} = \boldsymbol{p}_{k,t}^{u^{(a-1)}}$ in $\hat{R}_{ik,t}^{u^{(a)}}$ and $\hat{R}_{kj,t}^{d^{(a)}}$. Moreover,

$$\left.\frac{\partial \xi_{ik,t}^{u}}{\partial p_{ik}^{u}}\right|_{\boldsymbol{p}_{k,t}^{u}=\boldsymbol{p}_{k,t}^{u^{(a-1)}}} = \frac{g_{ik}^{u}}{2^{\xi_{ik,t}^{u}{}^{(a-1)}} \log_e 2} = \left.\frac{\partial \hat{R}_{kj,t}^{d}}{\partial p_{kj}^{d}}\right|_{\boldsymbol{p}_{k,t}^{u}=\boldsymbol{p}_{k,t}^{u^{(a-1)}}}$$

Hence, the proposed Algorithm 2 converges to a KKT point of the problem (**P2**) ∎

The optimality of the proposed SCA method is further complemented in simulation section through its performance comparison with optimal brute-force search for power allocation.

B. Optimal 3-D UAV Placement

In the previous subsection, the problem of optimal power allocation is solved with fixed 3-D UAV position. Nevertheless, the obtained rate-throughput from Algorithm 2 is the implicit function of UAV position, hence, it is required to find the optimal UAV position in order to secure maximum sum-rate throughput. With the given (or obtained from previous stage) power allocation, the problem of UAV placement for sum-rate maximization is formulated as

$$\begin{aligned}(\mathbf{P4}): \max_{\substack{\{r_{ik,t}^{u}\},\{p_{ik,t}^{u}\}\\ \{r_{kj,t}^{d}\},\{p_{kj,t}^{d}\}}} & \left\{\sum_{t=1}^{T_k}\left\{\sum_{i=1}^{I_{kt}} r_{ik,t}^{u} + \sum_{j=1}^{J_{kt}} r_{kj,t}^{d}\right\}\right\} \\ \text{s.t.} \quad & \text{(C3), (C4), (C5) of } (\mathbf{P1}), \\ & \text{(C6): } \log_2\left(1+\gamma_{ik,t}^{u}\right) \geq T_k r_{ik,t}^{u}, \\ & \quad i \in \boldsymbol{\mathcal{I}}_{kt}, t \in 1,\ldots,T_k, \\ & \text{(C7): } \log_2\left(1+\gamma_{kj,t}^{d}\right) \geq T_k r_{kj,t}^{d}, \\ & \quad j \in \boldsymbol{\mathcal{J}}_{kt}, t \in 1,\ldots,T_k. \end{aligned} \quad (41)$$

Similar to the problem (**P2**), (**P4**) is non-convex in nature due to non-concavity of (C6) and (C7) constraints. Specifically, the channel gain is non-linear function of UAV position due to which the equivalent relaxed concave form of LHS terms of (C6) and (C7) (or convex relaxation of the problem) becomes very hard to obtain [17], [27] and hence its convergence is not guaranteed. Therefore, we adopt two alternate methods to resolve this issue and to determine the optimal 3-D UAV positions: a) 3-D UAV BFS and b) UAV altitude BFS with fixed horizontal UAV placement. The BFS for optimal UAV placement execute exhaustive search method with fixed step size and solve the power allocation problem (**P3**) for numerous samples. The particular sample is selected as the optimal UAV position which gain maximum achievable sum-rate throughput. Let $\mathcal{R}_k(\mathbf{u}_k)$ denotes the converged sum-rate throughput obtained from Algorithm 2 at given initial UAV position $\mathbf{u}_k$. We then execute Algorithm 2 for varying values of UAV position $\mathbf{u}_k = [u_{x_k}, u_{y_k}, h_k]^T = \mathbf{u}_o$ such that $\mathbf{u}_o \in \left[\mathbf{u}^{\min}, \mathbf{u}^{\max}\right]$ and collect all the possible values of $\mathcal{R}_k(\mathbf{u}_o)$. The search algorithm is executed from $\mathbf{u}_k^{\min}$ to $\mathbf{u}_k^{\max}$ with fixed step size of $\mathbf{u}^s$. After completing this process, the optimal UAV position is selected among the best sum-rate throughput from all collected samples. The 3-D BFS particularly executes three-dimensional search and comparison operation which is although computationally complex, however, it ensure the optimal UAV position selection with optimal power allocation and maximum sum-rate throughput. Similar 1-D BFS procedure is executed for only UAV altitude BFS with $h_k \in \left[h^{\min}, h^{\max}\right]$ and h^s as the step size. Both the algorithms for optimal UAV selection is summarized in Algorithm 3. Following from the results in [32], the horizontal placement of each UAV is fixed at the respective cluster centroid in UAV altitude BFS. Nevertheless, the considered 2-D UAV placement problem in [32, see section III] involve minimizing the total path loss between its respective UNs. This problem is not although straightforward or equivalent to adopt for the problem (**P4**), however, it relaxes the hardness of the original optimal UAV placement problem. Moreover, it experiences reduced computational complexity as when compared with 3-D UAV BFS. The optimality of the both the algorithms is discussed shortly in the paper.

Algorithm 3 Optimal UAV Placement

A. 3-D UAV position BFS

1: **Input**: $\mathbf{u}_k^{\min}$ and $\mathbf{u}_k^{\max}$
2: Solve: $\mathcal{R}_k(\mathbf{u}_o), \forall \mathbf{u}_o \in \left[\mathbf{u}^{\min}, \left(\mathbf{u}^{\min}+\mathbf{u}^s\right), \left(\mathbf{u}^{\min}+2\mathbf{u}^s\right), \ldots, \mathbf{u}^{\max}\right]$ collect all $\mathcal{R}_k(\mathbf{u}_o)$ as $\{\mathcal{R}_k(\mathbf{u}_o)\}$
3: Solve: $\mathbf{u}_k = \max_{\mathbf{u}_o}\{\mathcal{R}_k(\mathbf{u}_o)\}$
4: **Output**: $\mathbf{u}_k$

B. Fixed Horizontal UAV placement and UAV altitude BFS

1: **Input**: $h^{\min}$ and $h^{\max}$
2: Solve: $\mathcal{R}_k(h_o), \forall h_o \in \left[h^{\min}, \left(h^{\min}+h^s\right), \left(h^{\min}+2h^s\right), \ldots, h^{\max}\right]$ collect all $\mathcal{R}_k(h_o)$ as $\{\mathcal{R}_k(h_o)\}$
3: Solve: $h_k = \max_{h_o}\{\mathcal{R}_k(h_o)\}$
4: **Output**: h_k

C. Computational Complexity

Here, we describe the overall computational complexity of the proposed method in this section. The proposed method is implemented in distributed fashion at each UAV i.e., the sub-clustering of UNs belonging to the particular UAV (cluster) and their power allocation and the UAV height determination is executed at the corresponding UAV concurrently. The computational complexity of elbow k-means algorithm implemented in t^{th} cluster is in the order of $O(N_k T_k M^{\max})$ where N_k is the total number of UNs in the t^{th} cluster and $M^{\max}$ is the maximum number of iterations in K-means algorithm until the convergence ($\phi_k^{(t+1)} = \phi_k^{(t)}$) is achieved. While, the final approximated power allocation problem obtained in (40) has $2(I_k + J_k)$ variables and $2I_k + J_k + 1$ constraints where $I_k = \sum_{t=1}^{T_k} I_{kt}, J_k = \sum_{t=1}^{T_k} J_{kt}$ and $N_k = I_k + J_k$. With consideration of worst case scenario, let the SCA algorithm converges at $L^{\max}$ iteration. The worst case computational complexity of SCA based power allocation algorithm is given by $O\left(L^{\max}\left(2(I_k+J_k)\right)^2(2I_k+J_k+1)\right)$. Further, the brute-force search algorithm or optimal 3-D UAV position considers $S_u^{\max} = \text{floor}\left(\frac{R\times R\times h^{\max}-h^{\min}}{(h^s)^3}\right)$ samples. However, the proposed solution with fixed horizontal placement and only UAV height determination execute the search operation for only $S_h^{\max} = \text{floor}\left(\frac{h^{\max}-h^{\min}}{h^s}\right)$. The BFS for all the variables

TABLE I
WORST CASE COMPUTATIONAL COMPLEXITY

Algorithm	Worst-Case Computational Complexity
First Stage Clustering	$O\left(NKM^{\max}\right)$
Second Stage Clustering	$O\left(N_k T_k M^{\max}\right)$
Proposed SCA	$O\left(4L^{\max}\left(I_k+J_k\right)^2\left(2I_k+J_k+1\right)\right)$
Proposed 3-D UAV BFS	$O\left(S_u^{\max}\right)$
Proposed UAV Height BFS	$O\left(S_h^{\max}\right)$
Power Allocation BFS	$O\left(\left(S_1^{\max}S_2^{\max}\right)^{\left(I_k+J_k\right)}\right)$
Joint BFS	$O\left(S_T^{\max}\right)$

with all the power and 3-D UAV position variables i.e., joint BFS involves total $S_T^{\max}=\left(S_1^{\max}S_2^{\max}\right)^{(I_k+J_k)}S_u^{\max}$ samples search operation where $S_1^{\max}$ and $S_2^{\max}$ are the samples for UL and DL power values, respectively. The optimal solution of BFS relies on the low step size, however, the decrease in step size significantly increases the sample size for BFS algorithms. For large scale network, the joint BFS becomes unreliable due to its very high computational complexity. The complexity of the proposed solution involving two-stage dynamic clustering, power allocation and optimal UAV placement is tabularized in Table I. The overall worst-case complexity of the proposed solution can be expressed as

$$O\Big(NKM^{\max}+N_kT_kM^{\max} +4S_u^{\max}L^{\max}\left(I_k+J_k\right)^2\left(2I_k+J_k+1\right)\Big), \quad (42)$$

where the first term $NM^{\max}$ signifies the first-stage user clustering. The overall complexity dominantly depends on the number of UNs belonging to the UAV. Intuitively, this implies that without clustering algorithm i.e., for single NOMA cluster, the worst case complexity of the proposed solution will significantly increase. The another important parameter affecting complexity of proposed solution is the convergence rate of the SCA algorithm. The fast convergence rate of the proposed SCA algorithm is validated shortly in the paper.

V. BASELINE OMA SCHEME

As a benchmark, we also considered conventional OMA for the designed framework i.e., time-division multiple access (TDMA) or time-division multiple access (FDMA) methods, where time/frequency resource allocation is non-adaptively and equally divided into all the UNs in the cluster. Now, the expression of r_{nk}^o for the n^{th} UN belonging to the k^{th} cluster for OMA scheme can be given as

$$r_{nk}^o=\frac{1}{N_k}\log_2\left(1+\frac{g_{nk}p_{nk}^o}{\sigma^2}\right), n\in\boldsymbol{\phi}_k \quad (43)$$

where p_{nk}^o is transmit power allocated to n^{th} UN and g_{nk} ($g_{nk}=g_{ik}^u$ or $g_{nk}=g_{kj}^d$) is the channel gain between the n^{th} UN (i^{th} UL or j^{th} DL) and k^{th} UAV. Similar to hybrid NOMA scheme, the problem of maximizing sum-rate throughput under power allocation for OMA scheme is expressed using slack variable, $\{r_{nk}^o\}$ as

$$\begin{aligned}(\mathbf{P5}): \max_{\{r_{nk}^o\},\{p_{nk}^o\}} \ & \sum\nolimits_{n\in\boldsymbol{\phi}_k} r_{nk}^o \\ \text{s.t.} \ & (\widetilde{C1}): p_{ik}^o\le p^{u,\max}, i\in\boldsymbol{\mathcal{I}}_k, \\ & (\widetilde{C2}): \sum\nolimits_{j\in\boldsymbol{\mathcal{J}}_k} p_{jk}^o\le p^{d,\max}, \\ & (\widetilde{C3}): \log_2\left(1+\frac{g_{nk}p_{nk}^o}{\sigma^2}\right) \\ & \ge N_k r_{nk}^o, n\in\boldsymbol{\phi}_k, \end{aligned} \quad (44)$$

where $(\widetilde{C1})$ and $(\widetilde{C2})$ denote the power budget for UL and DL nodes in OMA scheme, respectively. For any given values of $\{r_{nk}^o\}$, the objective function in (**P5**) is affine, while the constraint $(\widetilde{C1})$ and $(\widetilde{C2})$ are linear. Since, the LHS terms of constraints $(\widetilde{C2})$ in (**P5**) is logarithmic of affine functions which is concave, hence the constraint $(\widetilde{C3})$ is convex. Therefore, the problem (**P5**) is convex in terms of variables $\{p_{nk}^o\}$ and thus its solution can be obtained by solving this problem using standard convex optimization tools [45]. Similar to hybrid NOMA case, the optimal UAV position selection for OMA is executed using BFS.

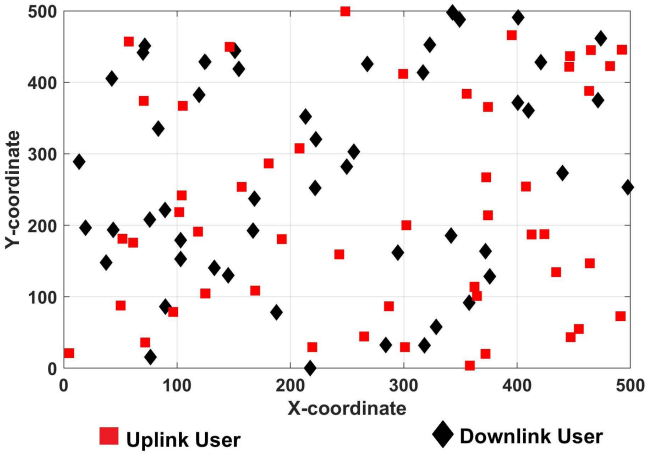

Fig. 4. Given network.

VI. NUMERICAL RESULTS AND DISCUSSIONS

In this section, the performance of the proposed FD enabled hybrid NOMA scheme is examined through extensive computer simulations. The simulations performances are averaged by 2000 Monte-Carlo simulations. For simulations, 100 UNs with 50 UL and 50 DL UNs are uniformly deployed on ground plane of 500×500 m^2 as shown in Fig. 4. The parameter settings are set as follows. Each UAV is equipped with two antennas for simultaneous transmission and reception which are separated by distance, $d_k^a=1$m and hence, operates in FD mode. Each user node is equipped with single antenna and operates in half-duplex mode. The RSI coefficient and the noise power are considered as $\tau=-100$ dB and $\sigma^2=-100$ dB, respectively. The channel coefficient for LOS and NLOS links are $\alpha_L=0.9$ and $\alpha_N=0.1$ and the path loss exponent of the network is $\gamma=3$. With an urban environment setting, the parameters ζ and β are set as 11.95 and 0.136,

TABLE II
PARAMETER SETTING FOR NETWORK SIMULATION

Parameter	Value	Parameter	Value
Number of UAVs, K	5	Number of UL UNs	50
Number of DL UNs ,	50	MSD Convergence, ϵ_c	0.1 m
Deployment Area, $R \times R$	500×500 m^2	Distance between UAV antenna, d_k^a	1 m
NLOS Attenuation, α_N	0.1	LOS Attenuation, α_L	0.9
Path Loss Exponent, γ	2	RSI Coefficient, τ	-100 dB
Lowest UAV Altitude, $\mathbf{u}^{\min}$	$[0, 0, 20]^{\mathrm{T}}$ m	Highest UAV Altitude, $\mathbf{u}^{\max}$	$[500, 500, 100]^{\mathrm{T}}$ m
UL Power Budget, $p^{u,\max}$	3 W	DL Power Budget, $p^{d,\max}$	25 W
Maximum SCI Iterations, $L^{\max}$	10	SCA Convergence Resolution, ϵ_r	0.01
Height step size, h^s	5 m	Noise variance, σ^2	-100 dB

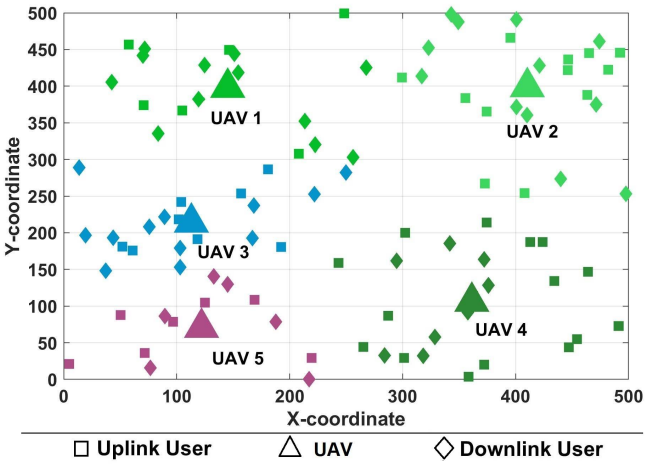

Fig. 5. 1st stage clustering.

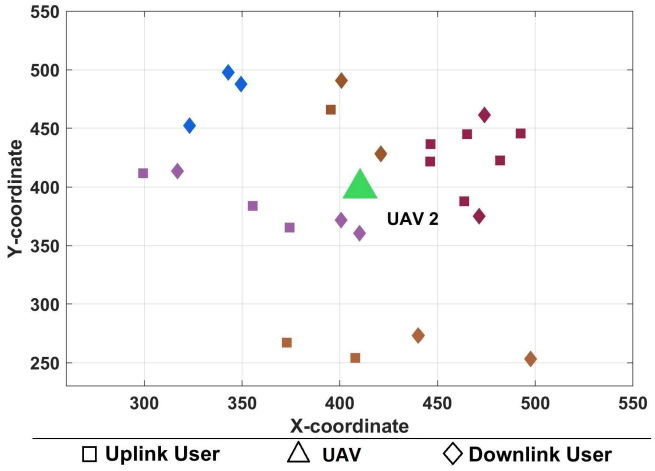

Fig. 6. 2nd stage clustering.

respectively [9]. The minimum QoS for UL and DL users are set as $\gamma^{u,\min} = 5$dB and $\gamma^{u,\min} = 10$dB, respectively [11]. The parameters setting considered for simulation is summarized in Table II. The UAV placement and power allocation problem is solved in distributed fashion on each respective UAV. We refer our proposed two-stage clustering based FD hybrid NOMA algorithm with UAV altitude BFS and 3-D UAV position BFS as TS-FDNOMA-1 and TS-FDNOMA-2, respectively in the rest of the paper. For SCA method, we initial transmit power for UL and DL rate. As performance benchmark for comparison, we simulate the conventional OMA i.e., we solve the problem (44) which is referred as OMA in the results. In addition to that we also highlight the effects and importance of dynamic clustering in the proposed method. We also analyze the performance behaviour of the proposed method with respect to a single stage clustering (SS-FDNOMA-2) i.e., without sub-clustering for considered framework. Moreover, we also consider HD-NOMA (referred as TS-HDNOMA-2) for the performance comparison.

For the given network, the proposed dynamic user clustering is illustrated in Fig. 5 and Fig. 6. The UL and DL UNs are denoted by square and diamond shapes, respectively. In the first stage, the UNs in the given network are clustered into 5 (i.e., equal to the number of UAVs). The UAV placed on the coordinates of the centroid. The triangle represent the horizontal UAV placement. Later, each cluster is again sub-clustered as considered for the cluster 2 as shown in Fig. 6. To illustrate the contrast between the proposed k-means based clustering and CSI based user clustering [11], [24] for the proposed FD-NOMA system, we analyze the performance comparison of both the clustering schemes with varying noise power σ^2 considering single stage clustering, 1 UAV, 10 UL UNs and 10 DL UNs. Note that the noise power here correspond to imperfect CSI information and other error propagation.

Fig. 7 demonstrate that the performance of the k-means based FD-NOMA (KM-SS-FDNOMA-2) is closer to the CSI based user clustering (CSI-SS-FDNOMA-2) for less imperfect (or nearly perfect) CSI acquisition. Importantly, the performance degradation of the proposed FD-NOMA system with CSI clustering for increased noise power is more serious than the k-means clustering. Intuitively, the CSI based clustering rely more on the perfect acquisition. Moreover, it is also found out that for the considered network, the average execution time (time-complexity) of proposed k-means clustering and CSI based clustering are nearly 0.3614 seconds and 0.5511 seconds, respectively. This clearly elucidate the motivation behind adopting the k-means based clustering.[5]

[5]The utilization of CSI information or hybrid clustering model involving both unsupervised and CSI based clustering is quite interesting. The detailed discussion of the impact of CSI based clustering on the considered resource allocation problem can be taken into account as near future research work as the extension of this work.

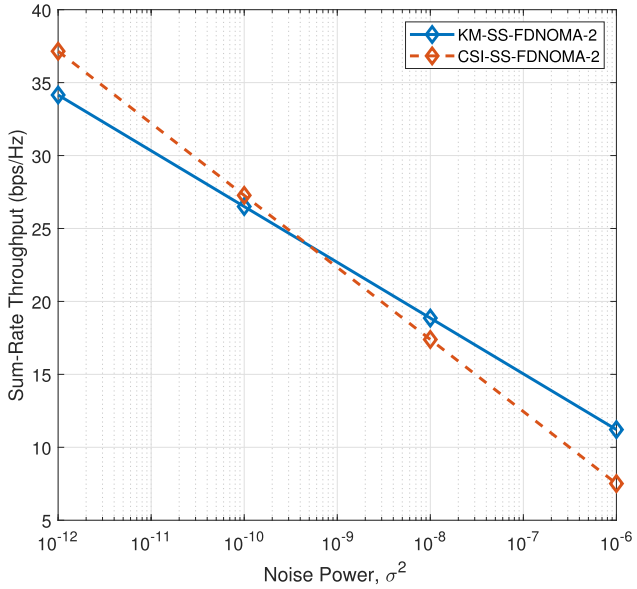

Fig. 7. Sum-Rate vs Noise power, σ^2.

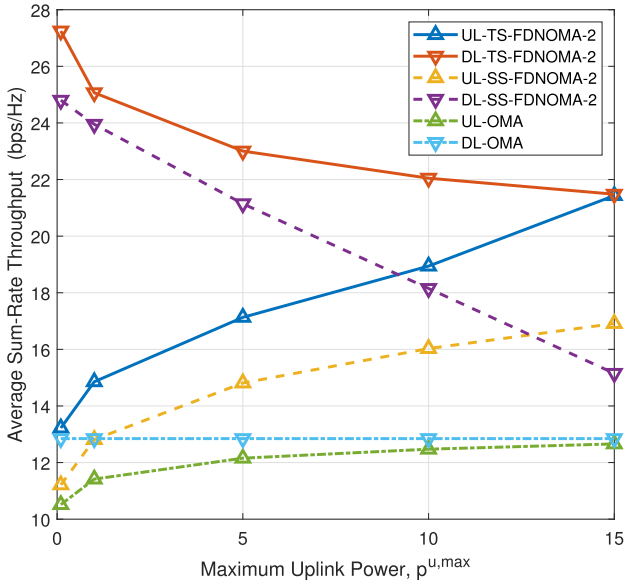

Fig. 9. Sum-Rate vs UL power budget, $p^{u,\max}$.

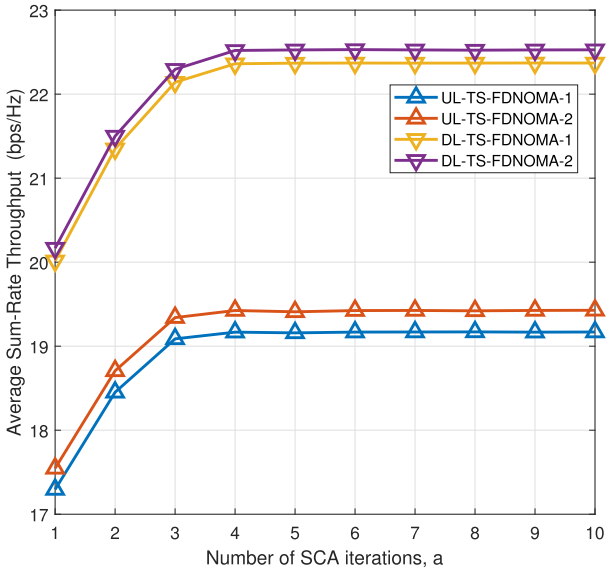

Fig. 8. Sum-Rate vs SCA iterations.

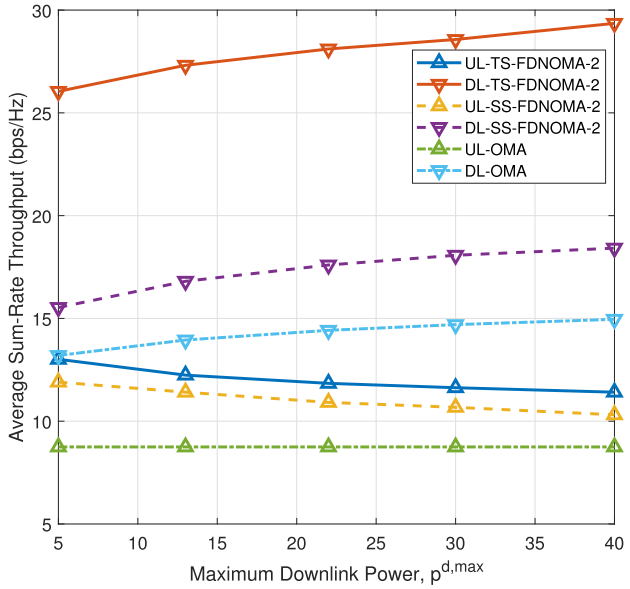

Fig. 10. Sum-Rate vs DL power budget, $p^{d,\max}$.

Firstly, we examine the convergence behaviour of the proposed methods with respect to SCA iterations. Fig. 8 shows the convergence behaviour of the proposed TS-FDNOMA-1 and TS-FDNOMA-2 methods with respect to the number of SCA iterations. Particularly, the TS-FDNOMA-2 perform slightly better TS-FDNOMA-1 due to the optimal UAV placement through 3-D BFS. We utilize the parameter setting mentioned in Table II and execute the SCA method with varying iterations. It can be observed that the average sum-rate for UL and DL UNs increases with the number of iterations and the proposed algorithm converges within four iterations. Next, we analyze the performance behavior of the proposed algorithm with respect to the UL and DL power budget. We simulate the considered methods for varying maximum UL power $p^{u,\max}$ and maximum DL power $p^{d,\max}$ as shown in Fig. 9 and Fig. 10, respectively. In Fig. 9, we can observe that the increase in $p^{u,\max}$ results in increase in UL rate. However, the DL rate for TS-FDNOMA-2 and SS-FDNOMA-2 decreases with the UL power $p^{u,\max}$ as the CCI increases significantly with increasing $p^{u,\max}$. For OMA case, the DL rate remains constant as CCI does not perturb the performance as illustrated in Fig. 9. Particularly, the rate of decrease of the DL rate in TS-FDNOMA-2 is lower than for SS-FDNOMA-2. It is due to the fact that the second stage dynamic sub-clustering reduces the effect CCI on DL transmission (although upto some extent only) and without sub-clustering the effect of CCI is comparatively higher in SS-FDNOMA-2. Similarly, in Fig. 10, it can be observed that with increase in $p^{d,\max}$, the DL rate improves significantly, however, the RSI does not alter the performance of

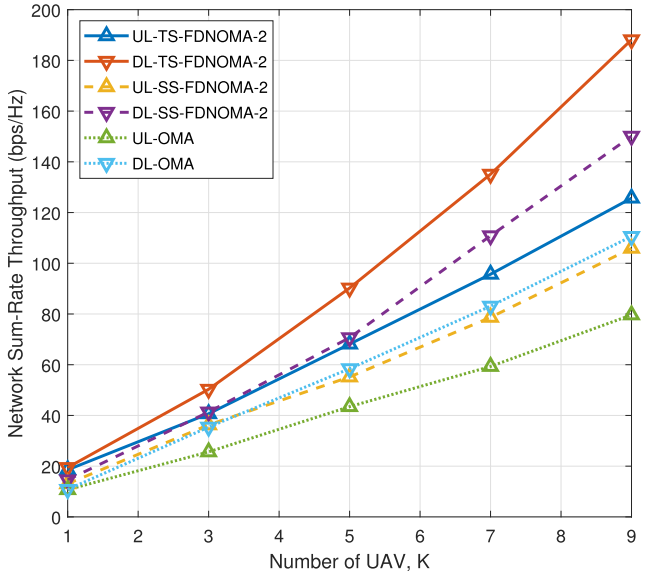

Fig. 11. Sum-Rate vs Number of UAV, K.

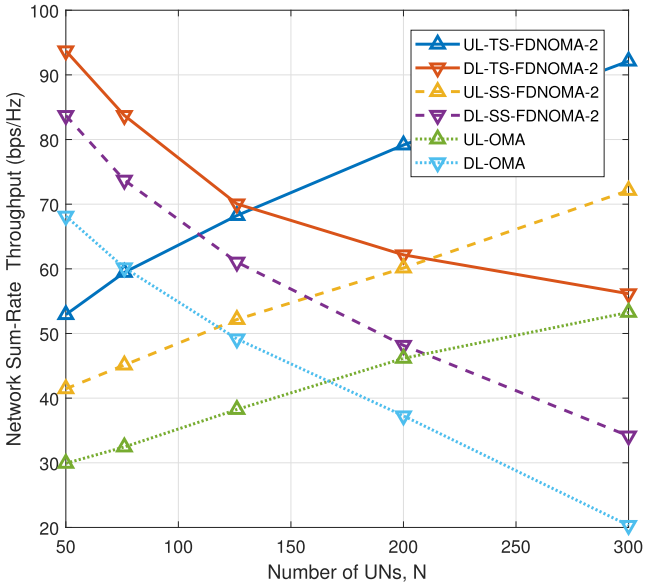

Fig. 12. Sum-Rate vs Number of UNs, N.

UL which remains almost constant for all the considered scenario. Notably, the effects of CCI are more in the DL as compared to RSI in UL transmission. Nevertheless, the effect of RSI depends upon RSI coefficient, τ. Overall, for both the scenarios, the proposed TS-FDNOMA-2 performs better with respect to UL and DL transmission when compared to SS-FDNOMA-2 and OMA schemes.

We also analyze the performance behavior of the proposed method with varying number of UAVs in the network as illustrated in Fig. 11. We fix the total number of UNs (with equal UL and DL UNs) and consider the total sum-rate throughput for all UL and DL UNs. The increase in UAVs decreases the UN density for each UAV which in turn maximizes the DL power allocation, reduces sub-clusters and minimizes cross-interference channels (CCI and RSI) and hence the overall network throughput increases [23]. For OMA case, the increase in UAV decreases the UN density (N_k) for each UAV and hence system throughput is improved. Moreover, the proposed TS-FDNOMA-2 and SS-FDNOMA-2 outperform OMA scheme.

In next scenario, we fix the UAVs and vary the number of UNs and examine the performance behaviour for the proposed algorithm as shown in Fig. 12. Since the total maximum DL power allocation for an UAV is fixed, the increase in total UNs results in reduced power allocation for each DL transmission and hence the sum-rate throughput for each DL UN decreases with increase in UNs. However, the same is not true for UL case. Unlike DL, the power allocation of UL UNs are constrained individually, moreover with increase in UN density each UL UN operates considerably with high power. Therefore, UL UNs remains considerably unaltered and overall rate for UL increases with increasing UL UN. The results in Fig. 11 and Fig. 12 consider equal UL and DL UN density. In practical scenarios, any cellular network experiences usual variations in UL and DL traffic. In the next scenario, we analyze the average sum-rate throughput

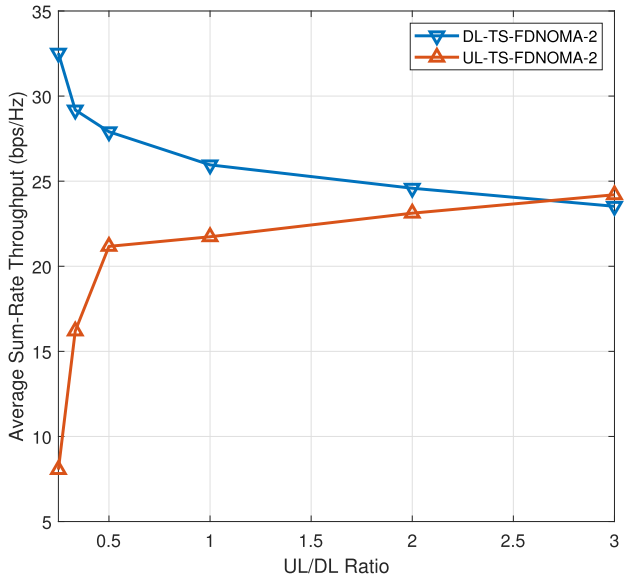

Fig. 13. Sum-Rate vs UL/DL Ratio, K.

for each UAV with varying number of UL and DL UNs (more specifically UL/DL UNs ratio in the network) as shown in Fig. 13. It is quite intuitive that with increase in UL UNs or with decrease in DL UNs, the average UL throughput per UAV increases due to increase in UL nodes (as discussed above) and reduction in the RSI [11]. However, due to increase in UL UNs the effect of CCI becomes significant for DL case and hence average DL rate for the cluster degrades.

Nextly, we compare the system performance of proposed multi-UAV FD-NOMA system with it equivalent single UAV system. Fig. 14. illustrate that the considered multi-UAV system (Multi-TS-FDNOMA-2) achieve better performance than single-UAV system (Sing-UAV-TS-FDNOMA-2) with high UN density. Particularly, the average rate throughput for the Sing-UAV-TS-FDNOMA-2 degrades more rapidly as compared to the Multi-UAV-TS-FDNOMA-2. It is due to the

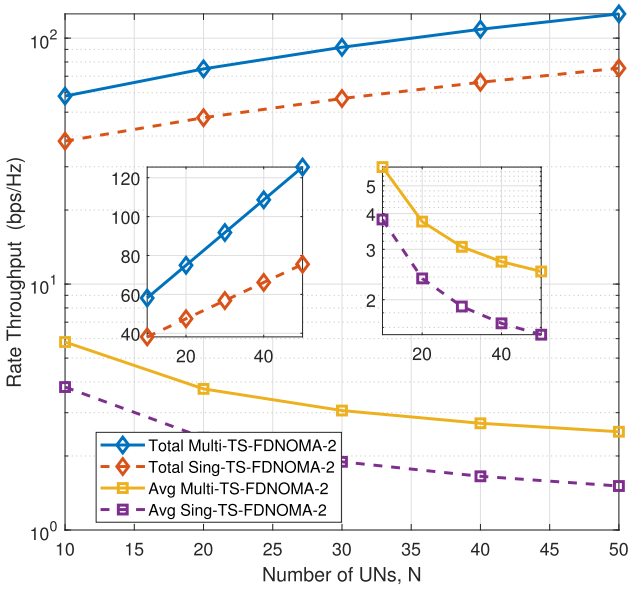

Fig. 14. Sum-Rate vs power coefficient, ρ.

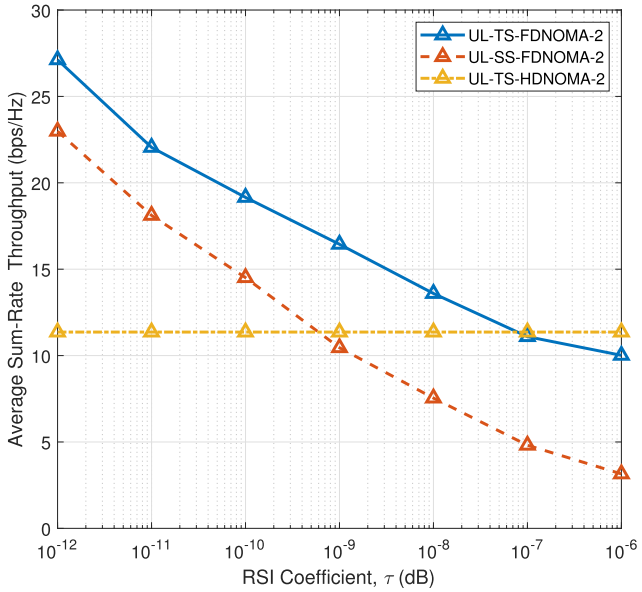

Fig. 15. Sum-Rate vs RSI coefficient, τ.

fact that the channel gain especially for the far users severely degrade in the single-UAV system. The considered multi-UAV deployment gain better coverage capability and improved sum-rate throughput for the system as when compared with the single UAV deployment.

We now demonstrate the behaviour of the proposed method and the effects of dynamic clustering with respect to the variation of RSI coefficient τ. Surely, the UL sum-rate for any FD-NOMA decreases with increases in the τ, however, the effect of SI (or RSI) is considerably less vulnerable for the proposed method when compared to the conventional single stage clustering as shown in Fig. 15. It is due to fact that the average RSI effect in the sub-cluster decreases as number of DL UNs decreases which is more favourable. As shown in Fig. 15, the performance of the proposed FD-NOMA scheme performs better low values of τ and especially it degrades

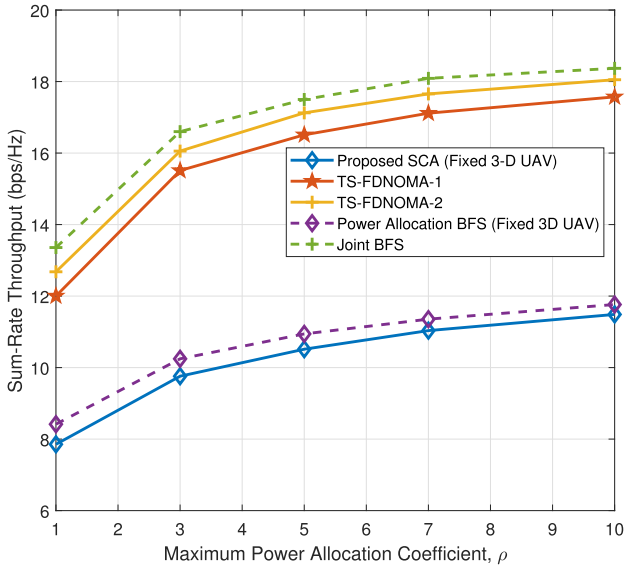

Fig. 16. Sum-Rate vs power coefficient, ρ.

over large values of τ ($> 10^{-7}$) as compared to HD-NOMA case. Hence, the proposed FD-NOMA scheme depends upon the appropriate SI mitigation techniques with RSI coefficient $\leq 10^{-7}$ which is not hard to obtain [38].

Nextly, we examine the overall sum-rate throughput of both the proposed solutions and the joint BFS solution for a small-scale network (including only 2 UL and 2 DL UNs, 1UAV and 1 sub-cluster) with respect to varying maximum power allocation coefficient ρ, where $p^{u,\max} = 0.4\rho$ and $p^{d,\max} = 1\rho$ as shown in Fig. 16. Moreover, we have also compared the proposed SCA based power allocation method with BFS power allocation with fixed 3-D UAV position. The BFS algorithm for power allocation and UAV position is executed with the step size of 0.15 watt and 1 meter, respectively. Importantly, the proposed low complexity SCA based algorithm attains a suboptimal solution which is closer to the optimal BFS with reduced complexity level as discussed earlier. Since the approximation in (36) and (37) are the upper bound approximation of the $\xi^u_{ik,t}$ and $\xi^d_{kj,t}$ (C6) and (C7), respectively, the solution obtained by Algorithm 2 is slightly suboptimal as compared to power allocation BFS with fixed UAV position as illustrated in Fig. 16. The proposed TS-FDNOMA-1 algorithm achieve performance closer to the optimal joint BFS algorithm. Intuitively, the proposed TS-FDNOMA-2 gain reduced computational complexity at the cost of slightly inferior overall rate throughput as compared with TS-FDNOMA-1. Nevertheless, the issue of trade-off between system performance and the computational complexity is most common for the resource allocation algorithm and there selection is application dependent. For large scale network with high UN density, the joint BFS search is no more reliable due to its high computational complexity and hence, the proposed sub-optimal algorithms with low complexity can be preferred.

VII. Conclusion

In this paper, we considered a multiple UAV-assisted FD NOMA based cellular network with aim to improve the overall throughput of the network. A two-stage unsupervised

user clustering algorithm was proposed in order to considerably reduce inter UAV interference and cross-interference i.e., SI and CCI in the considered FD-NOMA scheme. Further, we formulated a sum-rate maximization problem for each cluster under the optimal UL and DL power allocation and UAV placement. Due to non-convexity of the considered problem, we decoupled the original problem by addressing UAV placement and power allocation problem separately and first solved the power optimization problem iteratively using SCA method with fixed UAV position. We then utilized brute-force search algorithm to select the optimal UAV position which corresponds to maximum possible sum-rate throughput. Simulation results demonstrated that the proposed SCA method converges within four iterations and the proposed dynamic two-stage user clustering algorithm outperforms to conventional OMA and single stage user clustering schemes.

REFERENCES

[1] Y. Zeng, R. Zhang, and T. J. Lim, "Wireless communications with unmanned aerial vehicles: Opportunities and challenges," *IEEE Commun. Mag.*, vol. 54, no. 5, pp. 36–42, May 2016.

[2] L. Gupta, R. Jain, and G. Vaszkun, "Survey of important issues in UAV communication networks," *IEEE Commun. Surveys Tuts.*, vol. 18, no. 2, pp. 1123–1152, 2nd Quart., 2016.

[3] H. Wang, G. Ding, F. Gao, J. Chen, J. Wang, and L. Wang, "Power control in UAV-supported ultra dense networks: Communications, caching, and energy transfer," *IEEE Commun. Mag.*, vol. 56, no. 6, pp. 28–34, Jun. 2018.

[4] M. M. Azari, F. Rosas, and S. Pollin, "Cellular connectivity for UAVs: Network modeling, performance analysis, and design guidelines," *IEEE Trans. Wireless Commun.*, vol. 18, no. 7, pp. 3366–3381, Jul. 2019.

[5] W. Feng *et al.*, "NOMA-based UAV-aided networks for emergency communications," *China Commun.*, vol. 17, no. 11, pp. 54–66, Nov. 2020.

[6] A. V. Savkin and H. Huang, "Deployment of unmanned aerial vehicle base stations for optimal quality of coverage," *IEEE Wireless Commun. Lett.*, vol. 8, no. 1, pp. 321–324, Feb. 2019.

[7] L. Zhu, J. Zhang, Z. Xiao, X. Cao, D. O. Wu, and X. Xia, "Millimeter-wave NOMA with user grouping, power allocation and hybrid beamforming," *IEEE Trans. Wireless Commun.*, vol. 18, no. 11, pp. 5065–5079, Nov. 2019.

[8] L. Zhu, J. Zhang, Z. Xiao, X. Cao, X.-G. Xia, and R. Schober, "Millimeter-wave full-duplex UAV relay: Joint positioning, beamforming, and power control," *IEEE J. Sel. Areas Commun.*, vol. 38, no. 9, pp. 2057–2073, Sep. 2020.

[9] M. Mozaffari, W. Saad, M. Bennis, and M. Debbah, "Efficient deployment of multiple unmanned aerial vehicles for optimal wireless coverage," *IEEE Commun. Lett.*, vol. 20, no. 8, pp. 1647–1650, Aug. 2016.

[10] M. Mozaffari, W. Saad, M. Bennis, and M. Debbah, "Drone small cells in the clouds: Design, deployment and performance analysis," in *Proc. IEEE Global Commun. Conf. (GLOBECOM)*, Dec. 2015, pp. 1–6.

[11] K. Singh, K. Wang, S. Biswas, Z. Ding, F. A. Khan, and T. Ratnarajah, "Resource optimization in full duplex non-orthogonal multiple access systems," *IEEE Trans. Wireless Commun.*, vol. 18, no. 9, pp. 4312–4325, Sep. 2019.

[12] E. Park, J. Bae, H. Ju, and Y. Han, "Resource allocation for full-duplex systems with imperfect co-channel interference estimation," *IEEE Trans. Wireless Commun.*, vol. 18, no. 4, pp. 2388–2400, Apr. 2019.

[13] B. A. Jebur and C. C. Tsimenidis, "Impact of self and co-channel interference on an DNF full-duplex one-way relay system," in *Proc. IEEE Global Commun. Conf. (GLOBECOM)*, Dec. 2018, pp. 206–212.

[14] Z. H. E. Tan, A. S. Madhukumar, R. P. Sirigina, and A. K. Krishna, "NOMA-aided multi-UAV communications in full-duplex heterogeneous networks," *IEEE Syst. J.*, vol. 15, no. 2, pp. 2755–2766, Jun. 2020.

[15] A. A. Nasir, H. D. Tuan, T. Q. Duong, and H. V. Poor, "UAV-enabled communication using NOMA," *IEEE Trans. Commun. Mag.*, vol. 67, no. 7, pp. 5126–5138, Jul. 2019.

[16] Z. Chen, Z. Ding, X. Dai, and R. Zhang, "An optimization perspective of the superiority of NOMA compared to conventional OMA," *IEEE Trans. Signal Process.*, vol. 65, no. 19, pp. 5191–5202, Oct. 2017.

[17] Q. Chen, "Joint position and resource optimization for multi-UAV-aided relaying systems," *IEEE Access*, vol. 8, pp. 10403–10415, 2020.

[18] M. S. Ali, H. Tabassum, and E. Hossain, "Dynamic user clustering and power allocation for uplink and downlink non-orthogonal multiple access (NOMA) systems," *IEEE Access*, vol. 4, pp. 6325–6343, 2016.

[19] C. Shen, T.-H. Chang, J. Gong, Y. Zeng, and R. Zhang, "Multi-UAV interference coordination via joint trajectory and power control," *IEEE Trans. Signal Process.*, vol. 68, pp. 843–858, Jan. 2020.

[20] A. H. Gazestani, S. A. Ghorashi, Z. Yang, and M. Shikh-Bahaei, "Resource allocation in full-duplex UAV enabled multi small cell networks," *IEEE Trans. Mobile Comput.*, early access, Aug. 17, 2020, doi: 10.1109/TMC.2020.3017137.

[21] A. H. Gazestani, S. A. Ghorashi, Z. Yang, and M. Shikh-Bahaei, "Joint optimization of power and location in full-duplex UAV enabled systems," *IEEE Syst. J.*, early access, Nov. 23, 2021, doi: 10.1109/JSYST.2020.3036275.

[22] J. Cui, Z. Ding, P. Fan, and N. Al-Dhahir, "Unsupervised machine learning-based user clustering in millimeter-wave-NOMA systems," *IEEE Trans. Wireless Commun.*, vol. 17, no. 11, pp. 7425–7440, Nov. 2018.

[23] A. Celik, M.-C. Tsai, R. M. Radaydeh, F. S. Al-Qahtani, and M.-S. Alouini, "Distributed user clustering and resource allocation for imperfect NOMA in heterogeneous networks," *IEEE Trans. Commun.*, vol. 67, no. 10, pp. 7211–7227, Oct. 2019.

[24] K. Wang, W. Liang, Y. Yuan, Y. Liu, Z. Ma, and Z. Ding, "User clustering and power allocation for hybrid non-orthogonal multiple access systems," *IEEE Trans. Veh. Technol.*, vol. 68, no. 12, pp. 12052–12065, Oct. 2019.

[25] J. Plachy, Z. Becvar, P. Mach, R. Marik, and M. Vondra, "Joint positioning of flying base stations and association of users: Evolutionary-based approach," *IEEE Access*, vol. 7, pp. 11454–11463, 2019.

[26] J. Lyu, Y. Zeng, and R. Zhang, "UAV-aided offloading for cellular hotspot," *IEEE Trans. Wireless Commun.*, vol. 17, no. 6, pp. 3988–4001, Jun. 2018.

[27] M. A. Ali and A. Jamalipour, "UAV placement and power allocation in uplink and downlink operations of cellular network," *IEEE Trans. Commun.*, vol. 68, no. 7, pp. 4383–4393, Jul. 2020.

[28] C. Zhang, L. Zhang, L. Zhu, T. Zhang, Z. Xiao, and X.-G. Xia, "3D deployment of multiple UAV-mounted base stations for UAV communications," *IEEE Trans. Commun.*, vol. 69, no. 4, pp. 2473–2488, Apr. 2021.

[29] S. K. Singh, K. Agrawal, K. Singh, C. P. Li, and W. J. Huang, "On UAV selection and position-based throughput maximization in multi-UAV relaying networks," *IEEE Access*, vol. 8, pp. 144039–144050, 2020.

[30] Z. Xue, J. Wang, G. Ding, Q. Wu, Y. Lin, and T. A. Tsiftsis, "Device-to-device communications underlying UAV-supported social networking," *IEEE Access*, vol. 6, pp. 34488–34502, 2018.

[31] J. Wang *et al.*, "Multiple unmanned-aerial-vehicles deployment and user pairing for nonorthogonal multiple access schemes," *IEEE Internet Things J.*, vol. 8, no. 3, pp. 1883–1895, Feb. 2021.

[32] X. Liu *et al.*, "Placement and power allocation for NOMA-UAV networks," *IEEE Wireless Commun. Lett.*, vol. 8, no. 3, pp. 965–968, Jun. 2019.

[33] B. Li, S. Zhao, R. Zhang, and L. Yang, "Full-duplex UAV relaying for multiple user pairs," *IEEE Internet Things J.*, vol. 8, no. 6, pp. 4657–4667, Mar. 2021.

[34] H. V. Nguyen, V. Nguyen, O. A. Dobre, D. N. Nguyen, E. Dutkiewicz, and O. Shin, "Joint power control and user association for NOMA-based full-duplex systems," *IEEE Trans. Commun. Mag.*, vol. 67, no. 11, pp. 8037–8055, Aug. 2019.

[35] J. Cui, Z. Ding, and P. Fan, "Outage probability constrained MIMO-NOMA designs under imperfect CSI," *IEEE Trans. Wireless Commun.*, vol. 17, no. 12, pp. 8239–8255, Dec. 2018.

[36] A. Al-Hourani, S. Kandeepan, and S. Lardner, "Optimal LAP altitude for maximum coverage," *IEEE Wireless Commun. Lett.*, vol. 3, no. 6, pp. 569–572, Dec. 2014.

[37] "Propagation data and prediction methods for the design of terrestrial broadband millimetric radio access systems," ITU, Geneva, Switzerland, Tech. Rep., 2003.

[38] C. Motz, T. Paireder, H. Pretl, and M. Huemer, "A survey on self-interference cancellation in mobile LTE-A/5G FDD transceivers," *IEEE Trans. Circuits Syst. II, Exp. Briefs*, vol. 68, no. 3, pp. 823–829, Mar. 2021.

[39] X. Su, H. Yu, W. Kim, C. Choi, and D. Choi, "Interference cancellation for non-orthogonal multiple access used in future wireless mobile networks," *EURASIP J. Wireless Commun. Netw.*, vol. 2016, no. 1, p. 231, Dec. 2016.
[40] G. Raja, S. Anbalagan, A. Ganapathisubramaniyan, M. S. Selvakumar, A. K. Bashir, and S. Mumtaz, "Efficient and secured swarm pattern multi-UAV communication," *IEEE Trans. Veh. Technol.*, vol. 70, no. 7, pp. 7050–7058, Jul. 2021.
[41] J.-J. Wang, C.-X. Jiang, Z. Han, Y. Ren, R. G. Maunder, and L. Hanzo, "Taking drones to the next level: Cooperative distributed unmanned-aerial-vehicular networks for small and mini drones," *IEEE Veh. Technol. Mag.*, vol. 12, no. 3, pp. 73–82, Sep. 2017.
[42] H. T. Dao and S. Kim, "Power allocation for multiple user-type massive MIMO systems," *IEEE Trans. Veh. Technol.*, vol. 69, no. 10, pp. 10965–10974, Oct. 2020.
[43] J. Cui, Y. Liu, Z. Ding, P. Fan, and A. Nallanathan, "Optimal user scheduling and power allocation for millimeter wave NOMA systems," *IEEE Trans. Wireless Commun.*, vol. 17, no. 3, pp. 1502–1517, Mar. 2018.
[44] F. Fang, H. Zhang, J. Cheng, S. Roy, and V. C. M. Leung, "Joint user scheduling and power allocation optimization for energy-efficient NOMA systems with imperfect CSI," *IEEE J. Sel. Areas Commun.*, vol. 35, no. 12, pp. 2874–2885, Dec. 2017.
[45] S. Boyd, S. P. Boyd, and L. Vandenberghe, *Convex Optimization*. Cambridge, U.K.: Cambridge Univ. Press, 2004.
[46] M. Grant and S. Boyd. (2010). *CVX: MATLAB Software for Disciplined Convex Programming, Version 1.21*. [Online]. Available: http://cvxr.com/cvx
[47] Q. Shi, L. Liu, W. Xu, and R. Zhang, "Joint transmit beamforming and receive power splitting for MISO SWIPT systems," *IEEE Trans. Wireless Commun.*, vol. 13, no. 6, pp. 3269–3280, Jun. 2014.

Mayur Katwe (Graduate Student Member, IEEE) received the B.E. degree in electronics and telecommunication from the SGBAU University, Amravati, India, in 2013, and the M.Tech. degree in digital system from the Government College of Engineering, Pune, India, in 2016. He has submitted his Ph.D. thesis to VNIT, Nagpur, India, in 2021. He is currently a Post-Doctoral Researcher with the Institute of Communications Engineering, National Sun Yat-sen University (NSYSU), Taiwan. His current research interests include radio localization, full duplex radios, non-orthogonal multiple access, rate-splitting multiple access, intelligent reflecting surfaces, and unmanned aerial vehicles.

Keshav Singh (Member, IEEE) received the M.Sc. degree in information and telecommunications technologies from Athens Information Technology, Greece, in 2009, and the Ph.D. degree in communication engineering from the National Central University, Taiwan, in 2015. From 2016 to 2019, he was a Research Associate with the Institute of Digital Communications, University of Edinburgh, U.K. From 2019 to 2020, he was associated as a Research Fellow with the University College Dublin, Ireland. He currently works as an Assistant Professor with the Institute of Communications Engineering, National Sun Yat-sen University (NSYSU), Taiwan. His research interests include green communications, resource allocation, full-duplex radio, ultra-reliable low-latency communication, non-orthogonal multiple access, wireless edge caching, machine learning for communications, and large intelligent surface-assisted communications.

Prabhat Kumar Sharma (Senior Member, IEEE) received the B.Tech. degree in electronics and communication engineering from Uttar Pradesh Technical University, Lucknow, the M.Tech. degree in VLSI design from the Malaviya National Institute of Technology, Jaipur, and the Ph.D. degree in wireless communications from the University of Delhi in 2015.

He is currently an Assistant Professor with the Department of Electronics and Communication Engineering, Visvesvaraya National Institute of Technology, Nagpur, India. He has authored over 80 journal articles and conference papers. His current research interests include physical layer aspects of wireless, molecular and biological, and quantum communications. He was a recipient of Visvesvaraya Young Faculty Research Fellowship from the Ministry of Electronics and Information Technology, Government of India. He was awarded the URSI/InRaSS Young Indian Radio Scientist Award by the International Radio Science Union in 2019.

Chih-Peng Li (Fellow, IEEE) received the B.S. degree in physics from the National Tsing Hua University, Hsinchu, Taiwan, in June 1989, and the Ph.D. degree in electrical engineering from Cornell University, Ithaca, NY, USA, in December 1997.

From 1998 to 2000, he was a Member of Technical Staff with Lucent Technologies. From 2001 to 2002, he was a Manager of Acer Mobile Networks. Since 2002, he has been with the National Sun Yat-sen University (NSYSU), Kaohsiung, Taiwan, where he is currently a Distinguished Professor with the Institute of Communications Engineering. He has served various positions with NSYSU, including the Chairman of the Electrical Engineering Department, the VP of General Affairs, the Dean of the Engineering College, and the VP of Academic Affairs. His research interests include wireless communications, baseband signal processing, and data networks. He is also the Director General with the Engineering and Technologies Department, Ministry of Science and Technology, Taiwan. He is also the Chapter Chair of IEEE Broadcasting Technology Society Tainan Section. He has also served as the Chapter Chair for the IEEE Communication Society Tainan Section, the President for Taiwan Institute of Electrical and Electronics Engineering, the Editor for IEEE TRANSACTIONS ON WIRELESS COMMUNICATIONS, an Associate Editor for IEEE TRANSACTIONS ON BROADCASTING, the General Chair for 2020 Taiwan Telecommunications Annual Symposium, the General Co-Chair for 2017 IEEE Information Theory Workshop, the General Chair for 2014 IEEE 11th VTS Asia Pacific Wireless Communications Symposium, and the Member for Board of Governors with IEEE Tainan Section.

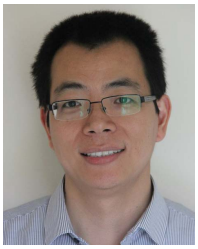

Zhiguo Ding (Fellow, IEEE) received the B.Eng. degree from Beijing University of Posts and Telecommunications in 2000, and the Ph.D. degree from Imperial College London in 2005.

From July 2005 to April 2018, he was working with Queen's University Belfast, Imperial College, Newcastle University, and Lancaster University. From October 2012 to September 2021, he was an Academic Visitor with Princeton University. Since April 2018, he has been a Professor of communications with The University of Manchester. His research interests include 5G networks, game theory, cooperative and energy harvesting networks, and statistical signal processing. He recently received the EU Marie Curie Fellowship 2012–2014, the Top IEEE TVT Editor 2017, IEEE Heinrich Hertz Award 2018, IEEE Jack Neubauer Memorial Award 2018, IEEE Best Signal Processing Letter Award 2018, and Friedrich Wilhelm Bessel Research Award 2020. He is serving as an Area Editor for the IEEE OPEN JOURNAL OF THE COMMUNICATIONS SOCIETY, an Editor for IEEE TRANSACTIONS ON VEHICULAR TECHNOLOGY, and was an Editor for IEEE WIRELESS COMMUNICATION LETTERS, IEEE TRANSACTIONS ON COMMUNICATIONS, and IEEE COMMUNICATION LETTERS from 2013 to 2016. He is a Distinguished Lecturer of IEEE ComSoc, and a Web of Science Highly Cited Researcher in two categories 2021.